Lawrence Berkeley National Laboratory
Recent Work

Title
Energy Dispersive X-Ray Fluorescence Analysis Using X-Ray Tube Excitation

Permalink
https://escholarship.org/uc/item/7b04k9dc

Authors
Jaklevic, J.M.
Giauque, R.D.

Publication Date
1992

eScholarship.org Powered by the California Digital Library
University of California

LBL-24769 c.2

Lawrence Berkeley Laboratory

UNIVERSITY OF CALIFORNIA

Engineering Division

To be published as a chapter in **Handbook on X-Ray Spectrometry: Methods and Techniques**, Marcel Dekker, Inc., New York, NY

RECEIVED
LAWRENCE
BERKELEY LABORATORY

AUG 5 1988

LIBRARY AND
DOCUMENTS SECTION

Energy Dispersive X-Ray Fluorescence Analysis Using X-Ray Tube Excitation

J.M. Jaklevic and R.D. Giauque

February 1988

TWO-WEEK LOAN COPY

This is a Library Circulating Copy which may be borrowed for two weeks.

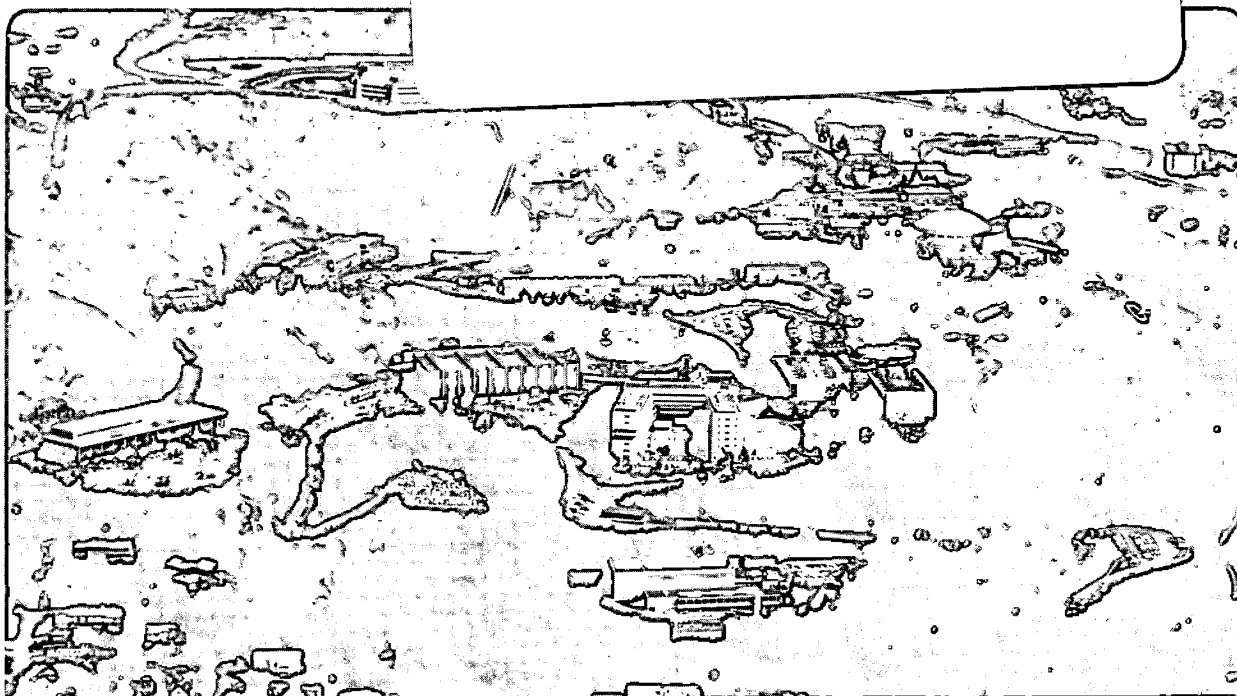

LBL-24769 c.2

Prepared for the U.S. Department of Energy under Contract Number DE-AC03-76SF00098.

DISCLAIMER

This document was prepared as an account of work sponsored by the United States Government. While this document is believed to contain correct information, neither the United States Government nor any agency thereof, nor the Regents of the University of California, nor any of their employees, makes any warranty, express or implied, or assumes any legal responsibility for the accuracy, completeness, or usefulness of any information, apparatus, product, or process disclosed, or represents that its use would not infringe privately owned rights. Reference herein to any specific commercial product, process, or service by its trade name, trademark, manufacturer, or otherwise, does not necessarily constitute or imply its endorsement, recommendation, or favoring by the United States Government or any agency thereof, or the Regents of the University of California. The views and opinions of authors expressed herein do not necessarily state or reflect those of the United States Government or any agency thereof or the Regents of the University of California.

LBL-24769

ENERGY DISPERSIVE X-RAY FLUORESCENCE ANALYSIS USING X-RAY TUBE EXCITATION*

Joseph M. Jaklevic and Robert D. Giauque

Lawrence Berkeley Laboratory
University of California
Berkeley, CA 94720 U.S.A.

February 1988

*This work was supported by the Director's Office of Energy Research, Office of Health and Environmental Research, U.S. Department of Energy under Contract No. DE-AC03-76SF00098.

TABLE OF CONTENTS

I. Introduction 1

II. Semiconductor Detectors for X-Ray Spectrometry 3

A. Detector Fabrication 4

B. Energy Resolution 6

C. Detector Efficiency 11

D. Detector Background 14

E. Count Rate Performance 16

F. Dead-Time Correction 20

G. Low Energy X-Ray Detection 22

III. X-Ray Tube Excitation 24

A. X-Ray Tube Design 25

IV. Applications of Tube-Excited X-Ray Fluorescence 32

A. Analysis of Liquids 33

B. Analysis of Solids 36

V. Summary 39

References 39

Figure Captions 43

ENERGY DISPERSIVE X-RAY FLUORESCENCE ANALYSIS
USING X-RAY TUBE EXCITATION

Joseph M. Jaklevic and Robert D. Giauque
Lawrence Berkeley Laboratory
University of California
Berkeley, CA 94720

I. Introduction

The term 'x-ray fluorescence analysis' (XRF) refers to the measurement of characteristic fluorescent emissions resulting from the de-excitation of inner shell vacancies which have been produced in the sample by means of a suitable source of radiation. Numerous variants of the basic process have been studied which differ in the type and source of ionizing radiation and in the method employed to measure the fluorescent emission.(1,2,3) For routine XRF analysis, two major approaches are distinguishable based on the type of detector used to measure the characteristics of the emission spectra. Wavelength dispersive (WD) analysis depends upon the use of a diffracting crystal to determine the characteristic wavelength of the emitted x-rays and is described in a previous chapter. Energy dispersive x-ray fluorescence analysis (EDXRF) employs detectors which directly measure the total energy of the x-rays by collecting the ionization produced in a suitable detecting medium.

Early approaches to EDXRF used gas proportional counters or scintillation detectors to determine the energy of the x-rays but were

limited in application because of the inherently poor energy resolution which precluded the separation of characteristic x-rays of adjacent elements in the periodic table. In the early 1970's the technology of solid state semiconductor diode detectors and associated pulse processing circuits was developed to the point where practical x-ray spectroscopy with an energy resolution of 200 eV or less became possible.(4,5,6) Although the energy resolution capabilities of semiconductor detectors remained inferior to that achieved by wavelength dispersive systems, the increased efficiency inherent in the energy dispersive method compensated in many analytical applications and permitted the use of a multiplicity of experimental geometries not practical with WDXRF. A wide variety of EDXRF analytical systems based on radioisotope sources, x-ray tubes, charged particle accelerators, microprobe electron beams, and synchrotron light sources have been developed in recent years and are the subject of this and succeeding chapters.

The introductory material in the present chapter discusses the instrumental aspects of the energy dispersive method with particular emphasis on the use of semiconductor spectrometers as the detecting element. Most of this material will be applicable to the discussions of related energy dispersive methods in later chapters. In addition, a detailed discussion of EDXRF analysis using laboratory x-ray tubes will be presented including applications. For a more complete discussion of the instrumental aspects of semiconductor detectors and associated electronics, the reader is referred to any one of a number of reviews on the topic.(7,8,9)

II. Semiconductor Detectors for X-Ray Spectrometry

Figure 1 illustrates the basic components involved in an EDXRF measurement. The excitation radiation consists of a suitable flux of ionizing radiation, i.e., photons, electrons, or heavy charged particles provided from one of many sources such as a radioisotope, x-ray tube, nuclear particle accelerator, or relativistic synchrotron beam. For x-ray fluorescence, the energy of the ionizing radiation must be sufficient to efficiently induce inner-shell vacancies in the atoms within the sample. For x-ray excitation, the incident energy must be above the binding energy of the ejected photoelectron. For electrons or heavy charged particles, the energy of the incident particle must be adequate to transfer the energy and momentum required to eject the atomic electrons from the bound state. This is typically 10 to 100 keV for electrons and several MeV for protons or heavier charged particles.

The sample is placed in the excitation flux and the fluorescent x-rays resulting from the de-excitation of inner shell vacancies are detected by the energy dispersive semiconductor spectrometer. In this type of detector, the total ionization produced by each x-ray striking the detector is converted to a voltage signal with amplitude proportional to the incident energy. Specially designed processing electronics are employed to maintain linearity of the voltage signal with respect to the original charge pulse. A multichannel analyzer accumulates an energy spectrum of the sequential events in a histogram memory. Since the energy analysis does not depend in any way upon the diffraction or focusing of the x-rays, the geometry of the system is

relatively insensitive to the placement of the detector with respect to the sample. This provides for a large solid angle and associated detection efficiency. Also, the mechanism by which the ionization signal is measured is not restricted to a narrow energy region thus allowing the simultaneous detection of x-rays over a wide dynamic range of the emission spectrum. The principal advantages of EDXRF derive from the capability for simultaneous detection of characteristic x-rays from multiple elements with high geometric efficiency.

A. Detector Fabrication

The energy dispersive detecting element is based on the simple semiconductor diode structure shown in Fig. 2. The example shown is a structure typical for Si(Li) detectors; however, the basic elements are similar for HPGe detectors. The device is fabricated on a cylindrical wafer of high quality semiconductor material with rectifying p^+ or n^+ contacts on opposing surfaces. The bulk of the material is characterized by a very low concentration of free charge carriers. This reduced free carrier concentration is achieved either with the use of extremely pure material in the case of high purity germanium detectors, HPGe, or through the charge compensation of p-type silicon with lithium donor atoms in the case of lithium-drifted detectors, such as Si(Li). A typical dimension for such a diode is 1 - 2 cm in diameter with a total thickness of 3 - 5 mm for the case of Si(Li) and 5 - 10 mm for Ge devices.

In the geometry shown, the lithium-diffused region acts as an n^+ contact; the metal surface barrier (typically a Au evaporation) serves as the p^+ rectifying contact. When the diode is reverse biased, any

remaining free carriers are swept out of the bulk by the applied field and an active depletion region is created. In this condition, the only current which flows between electrodes on the respective contacts is due to thermally generated charge carriers which are excited above the narrow band-gap of the semiconducting material.

When a x-ray photon is incident upon the active volume or depletion region of the diode, it will normally interact by photoelectric absorption to create an inner shell vacancy in the semiconductor material together with an energetic photoelectron. This photoelectron interacts with the atoms in the semiconductor crystal lattice to produce multiple low-energy ionization events. This process continues until the electron comes to rest at the end of a total range which is short compared with the dimensions of the crystal. The energy associated with the inner shell vacancy is likewise absorbed in the crystal in most cases following the emission of Auger electrons or multiple low energy x-rays and subsequent reabsorption. The result of these multiple ionization processes is the production of a large number of free electron-hole pairs in the sensitive volume of the diode structure. These free charge carriers are then collected by the applied field as a current pulse. The number of these carriers is directly proportional to the energy of the x-ray quantum incident on the detector.

The types of energy dispersive semiconductor x-ray spectrometers differ primarily in the properties of the material used to make the device. Although the most common materials for semiconductor detectors are silicon or germanium, devices based on the use of compound

semiconductors have also been fabricated and tested for specific applications.(10,11) Table 1 is a list of commonly used semiconductor materials together with values of parameters important for x-ray detector applications. In the following sections, the details of detector operation will be discussed with particular emphasis on those aspects which impact EDXRF most directly. These include the detector energy resolution, detection efficiency, spectral response, and system throughput.

B. Energy Resolution

The energy resolution of the semiconductor spectrometer system determines the ability of a given system to resolve characteristic x-rays from multiple-element samples and is normally defined as the full width at half maximum (FWHM) of the pulse height distribution measured for a monoenergetic x-ray at a particular energy. A convenient choice of x-ray energy at which resolution is quoted is the Mn K-alpha line at 5.932 keV since this emission is readily available from ^{55}Fe radioisotope sources. These x-rays are of sufficiently low energy that the contribution to the linewidth from the K-alpha doublet structure and the intrinsic radiation width of the emission lines can be neglected. This is not true for higher energy characteristic x-rays where the width of the emission line must be considered, particularly when precision spectral deconvolution is attempted. Figure 3 shows a typical pulse height spectrum of Mn x-rays taken simultaneously with a calibrated pulser input. The purpose of the pulser measurement is to monitor the resolution of the electronic system independent of any peak broadening due to the detector itself.

Typical state-of-the-art Si(Li) or HPGe detectors achieve FWHM of 175 eV at 5.9 keV although values as low as 160 eV have been reported. However, this number is but one indicator of the quality of an EDXRF detector system and other factors such as maximum count rate capability or the presence of background artifacts may be more important in many analytical applications.

If one neglects the intrinsic emission width of the x-ray lines, the instrumental energy resolution of a semiconductor detector x-ray spectrometer is a function of two independent factors. One is determined by the properties of the detector itself; the other is dependent upon the details of the electronic pulse processing employed. The FWHM of the x-ray line (ΔE_{total}) is described as the convolution of a contribution due solely to detector processes (ΔE_{det}) together with a component associated with limitations in the electronic pulse processing (ΔE_{elec}):

$$(\Delta E_{total})^2 = (\Delta E_{det})^2 + (\Delta E_{elec})^2 \qquad (1)$$

The detector contribution to the resolution (ΔE_{det}) is determined by the statistics of the free charge production process occurring in the depleted volume of the diode. The average number of electron hole pairs produced by an incident photon can be calculated as the total photon energy divided by the mean energy required to produce a single electron hole pair. If the fluctuation in this average was governed by Poisson statistics, then the variance would be the square root of that number. In semiconductor devices, the details of the energy loss

process are such that the individual events are not strictly independent and a departure from Poisson behavior is observed. This departure is taken into account by the addition of a Fano factor in the expression for the detector contribution to the FWHM.

$$(\Delta E_{det})^2 = (2.35)^2\ E\varepsilon F \tag{2}$$

where ε is the average energy required to produce a free electron-hole pair, E is the energy of the photon, and F is the Fano factor. E/ε is the total number of electron-hole pairs; the factor 2.35 converts the root mean square deviation to FWHM.

Examination of the values of ε and F listed in Table 1 shows that for an equivalent energy, the detector contribution to the resolution is 28% less for the case of Ge compared to Si. This could be an important consideration in the choice of detectors for certain experiments although this advantage of Ge over Si is mitigated in many applications because of the predominance of electronic noise at lower x-ray energies.

The contribution to resolution associated with electronic noise (ΔE_{elec}) is the result of random fluctuations in thermally-generated leakage currents within the detector itself and in the early stages of the amplifier components. Although these processes are intrinsic to the overall measurement process, there are methods for limiting the impact on the final system resolution. Figure 4 is a schematic diagram of a typical pulse processing system employed in a semiconductor detector x-ray spectrometer. The pulse processing can be divided between the charge integration, which takes place in the preamplifier, and the voltage amplification and pulse shaping, which

occur in the main amplifier. In order to achieve the noise performance necessary for x-ray fluorescence applications, the contribution of thermally-generated charge to the electronic noise is reduced by cooling the detector and the first stage of the preamplifier to cryogenic temperatures. This is normally performed using a liquid nitrogen reservoir in contact with a cold finger on which the detector and associated components are mounted. It has recently been demonstrated that noise performance adequate for many applications can likewise be achieved using thermoelectric coolers.(12,13)

The function of the charge-sensitive preamplifier and subsequent amplification stages is to convert the integrated charge pulse produced by the collection of the photoelectrically-induced ionization to a voltage pulse which can be measured and stored in the multichannel pulse height analyzer (MCA). However, the pulse processing must also achieve a very important goal of amplifying this weak charge signal to a measurable level while suppressing random fluctuations in the signal amplitude produced by thermal noise. This is achieved by generating a carefully defined pulse shape in the main amplifier which restricts the Fourier frequency components in the final signal in such a way that the signal contributions are emphasized relative to the noise fluctuations. The most common pulse shapers employed in modern semiconductor spectrometers generate output pulses which are gaussian, triangular or cusp shaped.(14,15,16) Each is capable of achieving adequate energy resolution for EDXRF analysis; the differences are due mainly to the effective time interval required to process a pulse. Since the relative amplitude of the noise contribution is a strong

function of the characteristic time constant associated with the pulse shaper, the difference between the types of shapers becomes important for applications in which high counting rates are important. For a careful evaluation of the differences associated with the various pulse shaping options, the reader is referred to (17).

The frequency distribution of the noise components in a typical x-ray spectrometer is illustrated in Fig. 5 in which the square of the deviation in the average number of thermally-generated ion pairs is plotted as a function of the characteristic peaking time of a simple pulse shaper. To calculate the noise in units of eV, the equivalent noise in electrons must be multiplied by the energy per ion pair given in Table 1. The solid lines show the contributions arising from two independent processes in the detector and in the first stage amplification elements. The dashed line is the sum of the two. The plots demonstrate that in general there exists a shaping time constant at which the contribution of electronic noise to the total resolution is a minimum. However, as will be pointed out later in the section on throughput, it is not always desirable to operate at this minimum noise shaping time since an unacceptably large dead time may result. Although modern commercial x-ray spectrometers are designed with a suitable compromise between energy resolution and count rate capabilities, an understanding of these tradeoffs on the part of the experimenter is important for optimum usage of the instrument.

Figure 6 summarizes the results of the energy resolution discussion by presenting plots of Eq. 1 as a function of energy for realistic detector types. Data for both Si and Ge have been calculated

based on parameters given in Table 1. It is clear from the plots that the energy resolution at low energies is influenced primarily by the electronic noise, whereas for energies above 10 keV, the detector properties dominate. Also, for this optimistic choice of detector properties, the Ge devices exhibit significantly better energy resolution due to the favorable average energy loss per ion pair and smaller Fano factor. Although energy resolution is one of the determining factors in one's ability to perform x-ray fluorescence analysis, it should be emphasized that there are other properties such as spectral background and counting rate capabilities that are equally critical when evaluating a given system for analytical applications.

C. Detector Efficiency

One of the more important advantages of semiconductor spectrometers is the absolute efficiency with which fluorescent x-rays are detected and their energies are measured. This is the result of the intrinsically high photoelectric absorption efficiencies for semiconductor materials in the x-ray energy range and from the large solid angles which are possible in typical fluorescence geometries. If one assumes a point source of x-rays and neglects edge effects around the detector periphery, then the total efficiency (ε) of a given geometry can be expressed as the product of the solid angle of the detector with respect to the sample and the intrinsic efficiency of the diode itself.

$$\varepsilon = \frac{\Omega}{4\pi}\,\varepsilon(E) \tag{3}$$

where Ω is the total solid angle and (ϵ) is the energy-dependent intrinsic efficiency of the detector. The solid angle is determined by the area of the detector and the sample-to-detector distance and varies with the design of the system. Typical areas are are 30 - 80 cm^2 for Si(Li) detectors and 80 - 320 cm^2 for HPGe detectors. Although the additional solid angle is advantageous for many applications, one must realize that the added capacitance associated with this area results in an increased contribution in the electronic noise of the system.

The intrinsic efficiency of the semiconductor device can be approximated by a simple model in which the probability of detecting an x-ray incident on the detector is assumed to be the probability of photoelectric absorption within the sensitive volume. This can be expressed as:

$$\epsilon(E) = e^{-\mu t}(1 - e^{-\sigma d}) \quad (4)$$

where t is the thickness of any absorptive layers between the sample and the detector, $\mu = \mu(E)$ is the mass absorption coefficient of the material, d is the detector thickness, and $\sigma = \sigma(E)$ is the photoelectric mass absorption coefficient for the detector material. Figure 7 shows plots of Eq. 4 for the case of a 3 mm thick Si(Li) and a 5 mm HPGe detector. The poor efficiency at low energies is assumed to be determined by the combined absorption of the 25 μm Be cryostat window and a nominal 2 cm air path between sample and detector. The energies of the characteristic K emission lines for several elements are also shown. The plots show the near unity intrinsic efficiencies for both detectors over a wide range of useful x-ray energies. The Ge

detector operates at much higher energies than Si due to higher atomic number and subsequent increase in photoelectric cross section.

This simple model gives a semi-quantitative picture of the efficiency behavior of semiconductor spectrometers. However, there are several other factors which must be considered for quantitative calibration of a fluorescence spectrometer. The concept of a thin entry window which either absorbs or transmits an incident x-ray does not describe cases where the secondary electrons, either photoelectric or Auger, are emitted into the active volume from the window layer. Similarly, detailed studies of the low energy efficiency have indicated the presence of an absorbing layer on the surface of both Si and Ge devices which is associated with the surface layer of the semiconductor material itself. Detailed experiments have indicated that the charge collection efficiency for events near the surface depends in a complex way upon low energy x-ray and charge transport properties.(18, 19) As a consequence of these entry-window-related effects, the efficiency for low energy photons can be reduced. The events lost from the photopeak can then appear in a continuum background below the full energy peak where they reduce detectability and interfere with spectral analysis.

Similarly, secondary electrons or photons originating from the photoelectric absorption events which occur initially in the active volume can escape. This results in a collected charge pulse of reduced amplitude. An easily observed manifestation of this involves the observation of discrete escape peaks in the spectrum. These are associated with the loss of a characteristic Si or Ge x-ray from the

active volume which produces a distinct peak in the spectrum at an energy the appropriate amount below the full energy peak. Continuous loss processes involving electron escape can also occur although the probability is small. These and related mechanisms which reduce the amplitude for a given event can lower the photopeak efficiency relative to the simple model described. There have been studies in which the efficiencies of Si(Li) and Ge have been carefully measured using calibrated sources of x-rays spanning the energy region of interest.(20,21,22) These indicate that the maximum intrinsic photopeak efficiency is reduced by a few percent relative to the curves shown in Fig. 7 and is slightly higher at the upper energy cutoff than calculated. These results substantiate the overall validity of the simple photoelectric absorption model but demonstrate the limitations if precise results are required. For most quantitative applications of EDXRF, it is not necessary to explicitly determine the photoelectric efficiency function since it is included in the overall calibration factor of the instrument.

D. Detector Background

Although artifacts associated with the partial collection of the photoelectric signal have a small effect upon the efficiency of the spectrometer, these processes can have far more serious consequences on analytical sensitivity through their effect upon spectral background. In cases where photon excitation is employed to induce fluorescence, there exist competing physical processes where the incident photons are scattered from the sample into the detector with very little loss in energy. These effects are particularly severe in trace

analysis applications where the number of matrix atoms which produce scattering is large compared to the number of fluorescence atoms. In these cases the major feature in the spectrum is a composite scatter peak consisting typically of a coherent and incoherent contributions. The effect of incomplete charge collection of these events is to produce a continuum of events at lower energies in the spectrum. These background events can then interfere with the measurement of lower energy fluorescent x-rays as shown in the schematic spectrum of Fig. 8. In this figure, the fluorescent x-rays are shown superimposed on a continuum background whose amplitude is proportional to the area of the composite coherent/incoherent scatttering peak at 17 keV. This background is the limiting factor in establishing the statistical accuracy in the determination of trace quantities.

Studies designed to reduce the source of this continuum background have indicated that in addition to fundamental x-ray and electron energy loss processes, a more significant background resulting from incomplete charge collection from the detector active volume is normally the dominant contribution.(23,24) This process is an artifact of the detector operation in which the collection of the free charge from the depleted volume is inhibited due to non-uniformities in the applied electric field associated with edge effects at the periphery of the cylindrical detector. The impact of this process on the quality of the spectrum can be reduced either by external collimators which prevent the incident radiation from interacting in the periphery of the device or by internal electronic collimation brought about by the use of a guard-ring structure.

E. Count Rate Performance

In many applications involving x-ray tubes or synchrotron sources, the available excitation intensity is sufficient to induce pulse counting rates which exceed the capabilities of the semiconductor spectrometer system. It then becomes necessary to reduce the excitation intensity or decrease the solid angle viewed by the detection system. Under most analytical applications, optimum performance is achieved when maximum throughput of events is maintained, although there are specialized applications where this is undesirable.

The count rate limitations associated with a semiconductor spectrometer are an inherent property associated with the finite pulse processing time required by the electronic shaping network. When a random sequence of pulses is incident on the detection system, some of the events cannot be processed without ambiguity. In order to appreciate the fundamental nature of this limitation and its relationship to system performance, some elementary concepts of electronic pulse processing must be considered.

Figure 9 illustrates the time sequence of pulses which occur at various stages in the pulse processing chain. Trace a) shows the output of the charge integrating preamplifier. The steps at times 1, 2,and 3 represent the charge integrals of discrete events. Traces b) and c) are the outputs of the fast (short shaping time) amplifier and an associated discriminator which serves as a timing marker for the individual events. The main shaping amplifier output is shown as the gaussian pulse shapes in trace d). For each event, a total pulse processing time (neglecting amplitude-to-digital conversion in the

pulse height analyzer) of τ_d is required after the arrival of the pulse before the system is ready to accept the next event.

Although the average counting rate detected by the system can be well below the frequency defined by the reciprocal of the pulse width τ_d, the fact that the events are statistically uncorrelated implies that the events are not uniformly distributed in time. There then exists a probability that two pulses will occur within the same processing time interval. This is illustrated by the overlap of pulses 2) and 3) in the trace.

At low average counting rate this overlap is not a limiting factor. However, as the average counting rate increases, a point is reached at which there is a significant probability that a second event will occur before the first has been fully analyzed. If the two events occur within a time less than the shaping time of the amplifier, the charge signals are indistinguishable and an erroneous "pile-up" energy signal will result.

Modern spectrometers employ some form of rejection circuitry in order to eliminate these pile-up events from the pulse height spectrum. Typical systems rely on the inspection of the fast discriminator output to determine if two pulses have occurred in rapid succession. Appropriate logic is then employed to gate the output of the processor in order to eliminate the resultant ambiguous energy signals. This is shown in e) and f) where the logic signal causes the output to be inhibited in the case where the pulses overlapped to produce an ambiguous energy output. Since the fast shaper which

generates the discriminator output has inherently poorer energy resolution relative to the slow channel, the pile-up rejection circuit is limited in the minimum energy pulses which it can detect. However, in typical photon-excited EDXRF where the major fraction of pulses occur from scattered high energy radiation, a pile-up rejector system is an important feature in the system design.

The pileup probability is obviously a function of the characteristic shaping time τ_p which in turn establishes the effective dead time of the system. This probability is independent of the details of the specific type of pile-up rejection circuit used to eliminate the ambiguous events. The number of events which experience pile-up and which are eliminated from the spectrum can be estimated for the case of a totally random arrival distribution. For a series of events which are randomly distributed in time with an average frequency N_o, the probability P that no pileup events occur within a characteristic time τ after a given event can be expressed as:

$$P = N_o e^{-N_o \tau} \tag{5}$$

From this expression, we can calculate the fraction of events which are transmitted through the system. Figure 10 is a plot of non-pile-up output rate vs. input rate expressed in terms of a characteristic pulse processing time. The input rate for which the output rate is a maximum is seen to be the reciprocal of the shaping time. The output rate at this point is a factor of 1/e less. It should be emphasized that this behavior is a fundamental consequence of random arrival statistics and a finite measurement time. However, one should be

aware that it is always possible to reduce the characteristic processing time in order to achieve an increase in counting rate at some sacrifice in energy resolution. For example, a typical pulse peaking time of 10 μs would imply a dead time of 20 μs and a maximum output rate of 18.4 kHz. If one were willing to sacrifice electronic resolution by reducing the shaping time to 2 μs peaking time, a maximum rate of 92 kHz would be possible. According to Fig. 5, this tradeoff would result in an increase in electronic noise from 100 eV to approximately 160 eV. If the application involved the detection of high energy x-rays, this compromise might be advantageous.

Although different algorithms can be used to correct for events lost to pile-up, there is no way to eliminate the effect through passive pulse processing.(25,26,27) Since different manufacturers of x-ray equipment vary in their approach to pile-up rejection, it is important to evaluate the throughput of the system using a variable intensity source of radiation. The input rate can be determined by scaling the fast discriminator output. The output rate can be simultaneously measured in the pulse height analyzer. A plot of non-pileup output rate vs. input rate can then be generated and compared to the ideal case shown in Fig. 10.

In cases where the excitation source can be switched off in a time interval which is short compared to the characteristic pulse processing time, it is possible to increase the average output counting rate by eliminating the effects of pile-up. Such pulsed excitation systems rely on the ability to detect an event in the fast channel and to shut off the excitation before a second pile-up event can occur. In this

mode of operation, the output rate can equal the input rate up to the point where the system is continuously busy, i.e., $N = 1/\tau$. This method of pile-up control has been implemented in several laboratories using pulsed x-ray tubes, particle accelerators, and electron probe beams.(28,29,30,31) In addition to increasing the maximum output counting rate, this method has the secondary advantage of reducing effects of heating in either the x-ray tube anode or the ion beam target since the excitation is turned off during the pulse processing interval.

Finally, it should be pointed out that there is a very important class of measurements in which the optimum counting rate is not achieved with maximum throughput. These are experiments such as fluorescence extended x-ray absorption fine structure (EXAFS) in which modulation of the x-ray yield is the quantity of interest.(32) Referring to Fig. 10, it is apparent that, at the maximum output rate, the slope is zero and, consequently, any modulation in the input rate will not affect the output rate. For EXAFS and similar applications, a lower input rate corresponding to a slope nearer unity is recommended.

F. Dead-Time Correction

The presence of pulse pile-up must be considered in any system designed for quantitative measurements since it causes the efficiency with which pulses are processed to be rate dependent. EDXRF analytical systems are designed to correct for this discrepancy through a variety of approaches. The most straightforward involve the use of a live-time clock consisting of a gated oscillator and scaler. The oscillator clock is turned off when the system is busy processing

pulses so that the duration of the measurement in terms of a live-time interval is corrected for those periods when the system is incapable of processing a pulse. Alternative methods rely on the direct measurement of the fast discriminator pulses in order to keep track of those events which were missed. An additional correction is added to compensate for those intervals in which pile-up is occurring.(33,34)

A simple empirical method for correcting for dead-time losses is to measure the ratio of input to output counts as a function of input rate over the range of values normally encountered. Subsequent analyses require that the input rate be measured for each experiment. The live-time correction can then be applied using the previously measured curve.

Since all live-time correction methods have some limitation on the range of counting rates over which they can be used, it is important that methods be devised to evaluate the precision with which such corrections are generated. A carefully prepared series of standards of varying concentrations represents a direct approach. A potentially more precise method involves the use of a single thin-film standard. Variable mass targets are placed behind the standard to vary the total counting rate over the range of interest. If the variable mass target is chosen so that the variable intensity of scattered or fluorescence radiation does not induce fluorescence in the thin-film standard, the measured intensity of fluorescence from the standard should be independent of total counting rate. The ability of the dead-time correction system to compensate for pile-up can then be empirically evaluated.

G. Low Energy X-Ray Detection

The efficiency curve shown in Fig. 7 illustrates that for conventional EDXRF measurements the absorption of fluorescent x-rays in air and in the Be entry window limits the accessible energy range to greater than 2 keV. This lower limit also corresponds to the energy range where other measurement artifacts associated with x-ray absorption such as matrix and particle size effects become significant. As a consequence, the necessity of a Be window to maintain vacuum integrity between the cryostat enclosure and atmospheric pressure does not constitute a serious limitation for most analyses. However, there do exist applications in which the detection of x-rays with energies below 1 keV becomes necessary particularly in microbeam analysis. It is therefore of interest to explore the fundamental limitations which semiconductor detector spectrometers exhibit in terms of subkilovolt x-ray detection.

If one neglects external sources of x-ray absorption, then the low-energy efficiency of a semiconductor detector is determined by the effective thickness of the entry window on the diode structure. This window is comprised of an evaporated contact used to form the rectifying Schottky barrier and a thin surface layer of inactive semiconductor material from which charge cannot be collected. The thickness of evaporated material, normally Au, can be determined by direct measurement during the manufacturing process and is typically in the range of 100 Å effective "dead layer" of semiconductor material is a more complicated parameter to determine. Empirical studies which have attempted to measure the absorption inherent in the semiconductor

surface layer have established that the effective thickness is determined to a large extent by the absorption length of the low energy photons and the charge transport characteristics of the associated ionization products. In the simplest model, there exists a competition between the rate of diffusion of the electron-hole distribution against the gradiant of the applied field. For distances near the entry contact, a part of the charge can diffuse into the contact and be lost to the signal before the electric field can sweep it to the opposing electrode. This loss of charge can be interpreted as the consequence of an effective "window" of typically 0.2 μm. Since this is an inherent charge transport property, it is not easily influenced through surface preparation of the semiconductor device. Figure 11 shows calculated efficiencies for the subkilovolt region assuming the typical values discussed above.(35) Absorption of both Au and Al contacts are illustrated as possible alternative choices for evaporated contact material. The results show that it is possible to measure x-ray energies down to the limits imposed by the noise of the counting electronics. Experiments have demonstrated the detection of x-rays as low as the k-alpha of Boron at 190 eV.(36,37)

In order to perform experiments at these low energies, it is obviously necessary to operate the system without the Be window interposed between sample and detector. This is typically done by including the sample and excitation source in the same vacuum enclosure as the detector. This introduces additional problems such as potential contamination on the detector window and the effect of low energy photons, i.e., optical fluorescence, on the detector output. Several

methods have been devised to address these problems involving the insertion of thin barriers between detector and sample within the same vacuum system. Because of the short mean free path of subkilovolt x-rays in any medium other than vacuum, the use of semiconductor detectors for the detection measurement of light elements remains largely limited to electron probe applications where the vacuum system is an inherent component of the measurement system and where the excitation process favors low atomic numbers.

III. X-Ray Tube Excitation

X-ray fluorescence using photons as an excitation source for inducing inner shell ionizations in the sample atoms is perhaps the most widely used method for EDXRF. Photons have the advantage of being readily available from either radioisotope sources or x-ray tubes. The mean free path of x-rays in the energy range of interest for chemical analysis is sufficient so that operation of the spectrometer in air is possible. Finally, the interaction of x-rays with the sample material is well understood and relatively insensitive to the chemical state of the specimen. It is thus possible to perform analyses with a minimum of sample preparation and with little concern for unknown matrix artifacts. A major disadvantage of photon excitation is the limited flux available from conventional sources and the difficulty in forming focused beams. However, with the increasing availability of synchrotron sources these latter objections are becoming less serious at least in large research laboratories where access to such facilities is possible.

Photon excitation with x-ray tubes continues to be the most practical method for routine EDXRF analysis. Compared with radioisotopes, the flux available with a typical low power x-ray tube is sufficient to provide for maximum counting rates for most applications. It is also possible to fluoresce secondary targets in order to generate high intensity fluxes of characteristic x-rays for monochromatic excitation. In contrast to a synchrotron source, the cost and size of a tube-excited system is consistent with operation in a typical analytical laboratory. In the following section the general features of x-ray tube excitation will be discussed and the relevant parameters determining the choice of excitation options will be described.

A. X-Ray Tube Design

The basic elements of an x-ray tube excitation system are shown in Fig. 12. The x-ray tube consists of a vacuum enclosure containing an electron source and target anode. A thin window is mounted in the vacuum wall to allow the x-rays to exit the tube enclosure. Commercial tubes are typically manufactured from glass although metal tubes with glass or ceramic electrical insulators are common.(38) The exit window is typically a thin mica or Be foil. The electron beam is generated using a thermionic cathode and is accelerated toward the anode by an electrostatic potential of 30 to 100 keV typically. In most applications the accelerating voltage is achieved with the anode assembly at ground potential with the insulated cathode assembly at the appropriate negative high voltage. This configuration is generally preferable since the thermal power generated in the anode by the

high energy electron beam can be more easily dissipated at ground potential.

The tube structure shown in the figure also has a control grid which can be used to modulate or pulse the emission current. This can be used to modulate the electron beam current in order to ensure constant output of radiation from the tube in DC operation or it can be used to rapidly switch the tube on and off for pulsed operation. In tubes without control grids, the output of the tube is maintained constant by regulating the temperature of the thermionic cathode. Reproducibility of analytical results is achieved for tube excitation by operating for a measured amount of time at a fixed emission current (DC operation) or for a fixed amount of integrated charge (pulsed operation). This approach depends upon the reasonable assumption that the total output x-ray flux is proportional to the number of electrons striking the anode.

The spectrum of x-rays produced in the anode is a continuum of energies upon which is superimposed the characteristic emission lines of the target material. The continuous x-ray "Bremsstrahlung" spectrum is the result of the slowing down of the electrons through interactions with the nuclear charges of the target atoms. This x-ray spectrum ranges from the lowest energies which can escape the anode target up to a maximum energy equal to the electron beam voltage. The characteristic x-rays are generated either through direct ionization of the target atoms by the incident electrons or through secondary excitation by photons in the high energy continuum. Figure 13 shows a schematic spectrum obtained from an x-ray tube with a Mo anode

(k-absorption edge at 20 keV) operated at 60 kV accelerating voltage. The step in the continuum distribution indicates the effect of self absorption by the target material for x-ray energies above the absorption edge.

The x-ray spectrum emitted by the anode can be used in any number of excitation and detection geometries. In Fig. 12 the beam marked (1) represents the configuration used for direct excitation of the sample by the x-rays emitted from the anode. A thin x-ray filter (typically the same element as the anode material) is used to preferentially transmit the characteristic x-rays generated in the anode. This configuration has the advantage of providing the most efficient use of the photons generated at the anode but has the disadvantage of lack of flexibility in choice of excitation energies.

In the second option shown, the sample is replaced by a secondary target whose characteristic x-ray spectrum is excited by the direct tube output. These x-rays are then incident on the sample. This geometry has the advantage of flexibility in the choice of excitation energies but does not make efficient use of the output flux. The total system efficiency is proportional to the product of the solid angle of the secondary target with respect to the anode times the solid angle of the sample with respect to the secondary target. Excitation geometries which make use of secondary targets must be carefully designed to achieve close coupling between the respective components without excessive scattering of direct, unfiltered radiation into the detector.

The third option is a variant of direct excitation in which the transmission of the x-rays through the anode itself is used to filter the continuum radiation. This method has certain advantages in the design of compact geometries particularly if the thin film anode is incorporated into the exit window. However, this design is limited in the amount of anode power dissipation which can be achieved in the anode structure.

In any of the excitation options chosen, the maximum flux available is limited by the amount of power which can be dissipated in the anode structure. X-ray tubes can be roughly classified according to the type of anode cooling employed. Low power x-ray tubes are typically air cooled and operate at a maximum of 100 watts at the anode. Tubes with water cooled anodes operate at 1000 watts. Rotating anode tubes can achieve 10 kilowatt dissipation. For a 50 kV anode potential, these ratings correspond to anode currents of 2, 20, and 200 ma respectively.

The yield of x-rays per incident electron is small since the majority of energy loss processes result in ionizations in the outer shell electrons from which little useful x-ray flux is derived. Calculations of the yield of characteristic and continuum photons for the case of typical anode materials is a difficult task since the details of the electron energy loss process and x-ray transport properties can be extremely complicated. However, for the purpose of acquiring order of magnitude estimates of total yields, approximate calculations can been made.(39,40,41) These are summarized in Table 2 for a number of anode materials. A convenient number to remember when

estimating fluorescent intensities of x-ray tube sources is that the the conversion efficiency for electron flux to either characteristic or continuum x-rays is approximately 1×10^{-5} photons/electron when the electron energy is three times the K shell binding energy of the anode material.

The choice of three times the K-shell binding energy is a recommended operating point for most applications in which the characteristic x-rays are the dominant source of excitation. For lower beam energies, the intensity of characteristic x-rays resulting from direct electron excitation has been calculated to vary as the 3/2 power of the applied anode voltage.(32) For beam energies much above the recommended value, the depth of penetration of the electron beam is sufficient that excessive x-ray absorption can occur. For secondary target systems, the voltage dependence is more complicated since it involves both the properties of the anode material and the secondary targets. Measurements performed using a Tungsten anode tube with a Mo secondary target have indicated the x-ray yield varies approximately as the square of the applied tube voltage.(42) In either case, it is important to realize that the excitation efficiency is affected by the beam voltage and that appropriate precautions must be taken to stabilize the applied voltage, particularly under variable current loads.

The choice of x-ray tube or excitation geometry is dictated largely by the analytical applications. For thick samples with heavy element matrices, maximum count rates can easily be achieved even with low incident excitation fluxes such as those obtained from a low power tube or an inefficient secondary target arrangement. For thin films

or trace element studies, more intense excitation fluxes are required. Finally, in specialized applications such as microbeam analysis, low background secondary target systems with inefficient geometries, or polarized scattering excitation(43,44,45,56), the elaboration of a rotating anode tube may be warranted.

For the majority of EDXRF applications, monochromatic x-rays (or nearly monochromatic characteristic x-rays) provide the most sensitive source for fluorescence excitation. This is because the maximum efficiency for photoabsorption in any given element is realized for incident energies immediately above the absorption edge of the particular element and decreases rapidly for higher energies. Furthermore, the flux of photons with energies below the edge produces no excitation but can interfere with the measurement of the fluorescent x-rays in the energy dispersive semiconductor detector. As a practical matter, the energy of the monoenergetic excitation is chosen sufficiently far above the absorption edge. Radiation which is elastically and inelastically scattered from the matrix does not overlap the photopeaks of the fluorescent x-rays.

Figure 14 shows the calculated efficiency for the production of inner shell vacancies for incident photon energies corresponding to three typical secondary target materials. The steep slope exhibited for atomic numbers below the maximum for each energy and the correspondingly narrow range of elements accessible for any one excitation energy demonstrate the desirability of multiple secondary targets for EDXRF.

Figures 15 and 16 illustrate the use of multiple excitation energies for the analysis of an air pollution sample consisting of a thin deposit of fine particles (diameter less than 2 μm) which have been collected from the ambient aerosol. The spectra were acquired using Mo K (17.4 and 19.6 keV) and Sm K (39.9 and 45.6 keV) secondary targets for excitation. The data are normalized to represent equal number of incident photons in each case. Note the order of magnitude difference in the vertical scale between the two spectra. Typical elemental concentrations (ng/cm^2) measured on this particular thin sample are: S = 15000, Fe = 2900, Cu = 60,Sr = 370, SB = 230 and Ba = 500. The Ta lines observed in the Sm excited spectrum are the result of collimator fluorescence.

For cases where optimum sensitivity for the detection of trace quantities is not necessary, the option of employing continuum excitation for uniform analytical sensitivity can be exploited. In this case, the fluorescence intensity does not depend strongly upon the energy of the absorption edge since a more or less continuous spectrum of excitation energies is available. However, since there also exists a continuum of energies available for scattering from the matrix, the minimum detectability for any element is reduced. An exception to this rule is for the case of the analysis of very light elements ($Z < 20$) where the additional flux together with the improved ratio of photoabsorption to scattering cross sections, combine to provide improved sensitivity for analysis even with continuum excitation.

IV. Applications of Tube-Excited X-Ray Fluorescence

Among the variety of implementations of EDXRF, tube excitation is probably the most versatile and most widely applied. The size and cost of a facility is appropriate for use in typical analytical laboratories and relatively high excitation fluxes can easily be achieved. For example, a 1 ma current in a typical x-ray tube produces the equivalent flux of a 500 Curie radioactive source. This excitation intensity is adequate to provide for analysis times of the order of 15 minutes duration even when secondary target geometries are employed. Although the stability of an x-ray tube cannot approach that of radioisotope sources, analytical precisions of 1% or less can typically be achieved for most tube-excited EDXRF applications.

Although radioisotope sources are limited in many applications due to lack of intensity, there are situations where they can be used to advantage. They can be designed for use in very compact geometries which compensates for the lower intensity. They are often used for portable EDXRF equipment where stringent power requirements must be met. Also, the range of energies available with radioisotope sources is not constrained by high voltage engineering considerations. Radioisotopes with characteristic emissions of 50 - 150 keV can be employed in conjunction with HPGe detectors to study the fluorescence from higher atomic number elements.

Recently, the use of synchrotron sources has become more extensively studied in EDXRF applications. Synchrotron emissions have the advantage that they are extremely intense, highly collimated, and polarized perpendicular to the beam direction. The ability to select

IV. Applications of Tube-Excited X-Ray Fluorescence

Among the variety of implementations of EDXRF, tube excitation is probably the most versatile and most widely applied. The size and cost of a facility is appropriate for use in typical analytical laboratories and relatively high excitation fluxes can easily be achieved. For example, a 1 ma current in a typical x-ray tube produces the equivalent flux of a 500 Curie radioactive source. This excitation intensity is adequate to provide for analysis times of the order of 15 minutes duration even when secondary target geometries are employed. Although the stability of an x-ray tube cannot approach that of radioisotope sources, analytical precisions of 1% or less can typically be achieved for most tube-excited EDXRF applications.

Although radioisotope sources are limited in many applications due to lack of intensity, there are situations where they can be used to advantage. They can be designed for use in very compact geometries which compensates for the lower intensity. They are often used for portable EDXRF equipment where stringent power requirements must be met. Also, the range of energies available with radioisotope sources is not constrained by high voltage engineering considerations. Radioisotopes with characteristic emissions of 50 - 150 keV can be employed in conjunction with HPGe detectors to study the fluorescence from higher atomic number elements.

Recently, the use of synchrotron sources has become more extensively studied in EDXRF applications. Synchrotron emissions have the advantage that they are extremely intense, highly collimated, and polarized perpendicular to the beam direction. The ability to select

a tunable band of wavelengths can be exploited to provide a near ideal excitation source which can provide excitation for small samples either directly or in a focusing geometry. The use of radioisotope and synchrotron sources are discussed in other chapters in this volume.

In the following section we discuss several analytical applications in which the use of x-ray tube-excited EDXRF has been prominent. In most cases the analysis could have been performed using alternative EDXRF procedures with appropriate consideration for differences in source intensity and counting times. In particular, when discussing sensitivities for tube-excited EDXRF, we choose as a typical analysis time interval 100 to 300 sec. Most photon-excited EDXRF analysis have in common much of the sample preparation, data acquisition, calibration and spectral analysis procedures. These are also the subjects of subsequent chapters.

A. Analysis of Liquids

Samples in the liquid form are homogeneous for XRF elemental determinations. For some industrial processes, the analysis of solutions is achieved using flow cells through which the concentrations of specific elements are closely monitored. These analyses can include the determination of trace and minor constituents of atomic number elements ($Z > 14$) in oils, gasolines, and aqueous solutions. If one or more characteristic x-ray lines from major or minor constituents do not completely dominate the spectrum, detection limits in the range of 1 to 10 μg/g can often easily be realized. Shown in Fig. 17 is a spectrum acquired from NBS SRM 1634 Fuel Oil. The element concentrations listed are in μg/g. The spectrum was acquired during a five-

minute count interval using excitation radiation from a low power Mo x-ray tube with external Mo filtering.

Sufficient sensitivities or selectivities often are not attainable to permit the direct determination of the elements in liquids. In these cases, the use of preconcentration procedures are required to reduce the matrix scattering. Some approaches that have been undertaken for the preconcentration of trace elements in waters and solutions include 1) evaporation, 2) precipitation of the desired elements followed by collection on a suitable thin substrate, 3) the application of cation and anion exchange resins and ion-collecting filters, 4) adsorption of elements onto activated carbon, and 5) chelation with subsequent sorption or solvent extraction. Most of the above approaches are capable of forming thin-film samples that are well-suited for multielement XRF determinations.

Preconcentration of elements by evaporation is an ideal approach in only limited cases. Often one or more elements such as sodium, calcium, or iron are present at much higher concentration levels than the desired elements to be determined. Evaporation can yield to fractional crystallization which, in turn, causes microscopically inhomogeneous residues. Furthermore, matrix effects may be considerably amplified. For relatively high purity liquids, a Mo high power x-ray tube has been used with a 0.4 mm x 0.8 mm optical focus to measure picogram quantities of trace elements.(47) A 50 μL portion of the liquid is dried on 4 μm polypropylene film for analysis.

Many elements in natural waters are organically bound in a variety of oxidation states. Pretreatment of the waters is then required

prior to preconcentraion. Also, for many waters, the concentrations of specific elements such as the alkali and alkaline earth elements are many orders of magnitude greater than the desired trace elements to be determined. Careful consideration must be given to approach undertaken to concentrate the elements. Ideally, the preconcentration procedure utilized should discriminate against the collection of the elements present at high concentrations so that high collection efficiencies can be realized for the desired trace elements.

Much of the early work on the precipitation of groups of elements for XRF determinations was done by Luke.(48) Extensive schemes for both general and selective precipitation of metal ions using a variety of reagents have been presented. Quantitative precipitation of a number of elements as a uniform deposit on thin filter substrate as achieved by the addition of a coprecipitant which served as a carrier. One reagent that was useful for the coprecipitation of a broad range of elements was sodium diethydthiocarbamate (carbamate). Dibenzyldithiocarbamate has a very low solubility in water and eliminates the need for a metal carrier. Near quantitative recoveries of Mn, Fe, Co, Ni, Cu, Zn, Se, Ag, Cd, Hg, Tl, and Pb have been demonstrated in a variety of water samples.(49) Detection limits of 1 - 5 μg/l for 100 ml samples were realized.

Anion and cation exchange resins also have been used to preconcentrate elements from aqueous solutions for XRF determinations.(50) The analysis of seawater for trace elements presents a particular challenge because the ratio of the major cations (Na, K, Ca, and Mg) exceeds the trace element content by a factor of 10^9. To overcome

a tunable band of wavelengths can be exploited to provide a near ideal excitation source which can provide excitation for small samples either directly or in a focusing geometry. The use of radioisotope and synchrotron sources are discussed in other chapters in this volume.

In the following section we discuss several analytical applications in which the use of x-ray tube-excited EDXRF has been prominent. In most cases the analysis could have been performed using alternative EDXRF procedures with appropriate consideration for differences in source intensity and counting times. In particular, when discussing sensitivities for tube-excited EDXRF, we choose as a typical analysis time interval 100 to 300 sec. Most photon-excited EDXRF analysis have in common much of the sample preparation, data acquisition, calibration and spectral analysis procedures. These are also the subjects of subsequent chapters.

A. Analysis of Liquids

Samples in the liquid form are homogeneous for XRF elemental determinations. For some industrial processes, the analysis of solutions is achieved using flow cells through which the concentrations of specific elements are closely monitored. These analyses can include the determination of trace and minor constituents of atomic number elements ($Z > 14$) in oils, gasolines, and aqueous solutions. If one or more characteristic x-ray lines from major or minor constituents do not completely dominate the spectrum, detection limits in the range of 1 to 10 μg/g can often easily be realized. Shown in Fig. 17 is a spectrum acquired from NBS SRM 1634 Fuel Oil. The element concentrations listed are in μg/g. The spectrum was acquired during a five-

minute count interval using excitation radiation from a low power Mo x-ray tube with external Mo filtering.

Sufficient sensitivities or selectivities often are not attainable to permit the direct determination of the elements in liquids. In these cases, the use of preconcentration procedures are required to reduce the matrix scattering. Some approaches that have been undertaken for the preconcentration of trace elements in waters and solutions include 1) evaporation, 2) precipitation of the desired elements followed by collection on a suitable thin substrate, 3) the application of cation and anion exchange resins and ion-collecting filters, 4) adsorption of elements onto activated carbon, and 5) chelation with subsequent sorption or solvent extraction. Most of the above approaches are capable of forming thin-film samples that are well-suited for multielement XRF determinations.

Preconcentration of elements by evaporation is an ideal approach in only limited cases. Often one or more elements such as sodium, calcium, or iron are present at much higher concentration levels than the desired elements to be determined. Evaporation can yield to fractional crystallization which, in turn, causes microscopically inhomogeneous residues. Furthermore, matrix effects may be considerably amplified. For relatively high purity liquids, a Mo high power x-ray tube has been used with a 0.4 mm x 0.8 mm optical focus to measure picogram quantities of trace elements.(47) A 50 μL portion of the liquid is dried on 4 μm polypropylene film for analysis.

Many elements in natural waters are organically bound in a variety of oxidation states. Pretreatment of the waters is then required

prior to preconcentraion. Also, for many waters, the concentrations of specific elements such as the alkali and alkaline earth elements are many orders of magnitude greater than the desired trace elements to be determined. Careful consideration must be given to approach undertaken to concentrate the elements. Ideally, the preconcentration procedure utilized should discriminate against the collection of the elements present at high concentrations so that high collection efficiencies can be realized for the desired trace elements.

Much of the early work on the precipitation of groups of elements for XRF determinations was done by Luke.(48) Extensive schemes for both general and selective precipitation of metal ions using a variety of reagents have been presented. Quantitative precipitation of a number of elements as a uniform deposit on thin filter substrate as achieved by the addition of a coprecipitant which served as a carrier. One reagent that was useful for the coprecipitation of a broad range of elements was sodium diethydthiocarbamate (carbamate). Dibenzyldithiocarbamate has a very low solubility in water and eliminates the need for a metal carrier. Near quantitative recoveries of Mn, Fe, Co, Ni, Cu, Zn, Se, Ag, Cd, Hg, Tl, and Pb have been demonstrated in a variety of water samples.(49) Detection limits of 1 - 5 μg/l for 100 ml samples were realized.

Anion and cation exchange resins also have been used to preconcentrate elements from aqueous solutions for XRF determinations.(50) The analysis of seawater for trace elements presents a particular challenge because the ratio of the major cations (Na, K, Ca, and Mg) exceeds the trace element content by a factor of 10^9. To overcome

the problem of the relatively low exchange capacity of resin-loaded filter papers, an indirect approach has been used for the analysis of Mn, Ni, Cu, Zn, and Pb at the 1 - 5 μg/l level.(51) A liter of seawater was initially passed through a Chelex-100 resin column. The trace metals were eluted from the resin column with a HNO_3 acid wash. The eluate was evaporated and heated to sublime the ammonium salts. Subsequently, the trace metals were taken into solution with acid and the metals were collected on SA-2 resin-loaded filter papers.

Preconcentration methods employed for the determination of trace elements in water by x-ray fluorescence have been reviewed by several authors. (49,52, 53) A wide variety of preconcentration methods is discussed and optimum conditions are evaluated. Some of the methods can be used for the preconcentration of certain metals when they are present in specific oxidation states only.

Preconcentration procedures employed for biological fluids include evaporation and lypholization. Also, dry and wet ashing techniques are utilized when further preconcentration of trace elements is required.

B. Analysis of Solids

X-ray tube systems are used for the determination of major, minor, and some trace elements in metals, alloys, steels, catalysts, and chemical compounds. In many cases, count rate limitations are easily imposed on the semiconductor detection system by high x-ray intensities from major or minor element constituents. This, in turn, can dictate sensitivities that are attainable. In some cases, the use of x-ray absorbing filters, placed between the sample and the detector,

can be used to preferentially reduce high intensity signals from major elements. This condition exists when major elements give rise to x-rays lower in energy than the desired weak higher energy signals. The use of photons provided by selected secondary targets whose fluorescence x-rays are not of sufficient energy to excite characteristic x-rays from some of the major constituents is often a good approach to improve analytical sensitivities. In the direct excitation mode, this same effect can also be achieved to some degree by optimization of the x-ray tube voltage chosen. For the determination of lower atomic number elements in alloys, highly polished sample surfaces are required. For many elemental determinations, high precisions are easily achieved.

A number of papers have been published regarding the use of x-ray tube excitation for broad range multielement determinations for sediments, clays, soils, minerals, cements, ores, and flyash. In some cases, pulverization and pelletization is the only sample preparation technique used. For the accurate determination of major elements (Na-Fe), the pulverized samples are usually fused with lithium metaborate-tetraborate mixtures or some similar type of mixtures. The resulting glass samples are homogeneous for the determination of the lower atomic number elements. Optimum conditions for the determination of both major and trace elements in silicate rocks have been developed.(54) Excitation radiation is provided directly by a pulsed low power Ag anode x-ray tube. Measurements are carried out in vacuum. The x-ray tube is operated at 10 kV for the determination of the elements Na to Fe in fused glass discs. Pellets prepared from

pulverized rock material are used for the determination of the trace elements. For these later measurements, an external Ag filter is employed and the x-ray tube is operated at 45 KV. The use of the Ag filter substantially enhances the signal-to-background ratios realized. A high degree of accuracy and precision is achieved for a wide range of major and trace elements. Limits of determination for many trace elements are in the range of 4 - 10 μg/g.

Tissues, plant materials, dried biological fluids are generally pulverized prior to analysis. In some cases, small quantities of the samples are spread on a thin substrate and the inelastic Compton scattered radiation intensity is used as a measure of the sample mass in the beam path. For the accurate determination of a broad range of trace elements, the pulverized samples are pressed into thin pellets. Sensitivities in the range of 0.5 - 10 ppm are often realized for higher atomic number elements ($Z > 20$) using count intervals of ten minutes or less. Using a low power Mo x-ray tube, a total of 22 elements were measured in light element matrices.(55) Results ascertained for NBS SRM 1571 Orchard Leaves are listed in Table 2. When x-ray counting statistics are not the limiting factor, results determined for many biological samples are typically accurate to within ± 10%.

Multilayer thin films, coatings, and air particulates collected on thin substrates are analyzed directly. Generally, two to four excitation conditions are chosen to achieve high sensitivities for a broad range of elements. Included with these excitation conditions is the use of transmission filters or secondary targets. Maximum signal-to-

background ratios are realized if the materials are collected on very thin low atomic number substrates ($Z < 10$), and if the samples are analyzed in vacuum or within a helium atmosphere. Using an x-ray spectrometer that employed a W-anode pulsed tube and three secondary targets, high sensitivities have been achieved for the analysis of aerosols collected on filters of mass < 1 mg/cm^2.(42) Samples are analyzed in a helium atmosphere. Table 3 lists the detection limits for 34 elements determined with this system.

V. Summary

The technology which makes chemical analysis with EDXRF practical is based on the use of semiconductor X-ray detectors and associated pulse processing and data acquisition electronic components. The present chapter has attempted to explain to the analyst the basic concepts behind the operation of these components and the manner in which they influence overall system performance. The tradeoffs which one must make between parameters such as detector resolution, count rate, excitation efficiency and other design variables determine how effectively one can tailor a given instrument or experimental apparatus to a specific application. Furthermore, a thorough understanding of the factors which limit performance should enable one to implement experimental tests to determine the effectiveness of a particular approach and evaluate various commercial options.

References

1. R. Jenkins, An Introduction to X-Ray Spectrometry, Heyden and Son, New York (1974).

2. H. A. Leibhatsky, H. G. Pfeiffer, E. H. Winslow, and P. D. Zemany, X-Rays, Electrons, and Analytical Chemistry, Wiley-Interscience, New York (1972).

3. E. P. Bertin, Principles and Practice of X-Ray Spectrometric Analysis, 2nd ed., Plenum Press, New York (1975).

4. E. Elad and M. Nakamura Nucl. Instr. and Meth., 41: 161 (1966).

5. H. R. Bowman, Science, 151: 562 (1966).

6. D. A. Landis, F. S. Goulding, R. H. Pehl, and J. T. Walton, IEEE Trans. Nucl. Sci., 18: 115 (1971).

7. G. F. Knoll, Radiation Detection and Measurement, John Wiley and Sons, New York (1979).

8. F. S. Goulding and D. A. Landis, "Semiconductor Detector Spectrometer Electronics" in Nuclear Spectroscopy and Reactions, Part A, Academic Press, New York (1974).

9. E. E. Haller and F. S. Goulding, "Nuclear Radiation Detectors" in Handbook on Semiconductors, Vol. 4, (C. Hilsson, ed.), North Holland (1981).

10. D. E. Leyden, A. R. Harding, and K. Goldbach, Adv. X-Ray Anal., 27: 527 (1984).

11. W. K. Warburton and J. S. Iwanczyk, Nucl. Instr. and Meth. in Phys. Res., A254, 123 (1987).

12. N. W. Madden. J. M. Jaklevic, J. T. Walton, and C. E. Wiegand, Nucl. Instr. and Meth., 159: 337 (1979).

13. N. W. Madden, G. Hanepen, ad B. C. Clark, IEEE Trans. Nucl. Sci., 33: 303 (1986).

14. E. Fairstein and J. Hahn, Nucleonics, 23: 50 (1965).

15. K. Kandiah, A. J. Smith, and G. White, IEEE Trans. Nucl. Sci., 22: 2058 (1972).

16. D. A. Landis, C. P. Cork, N. W. Madden, and F. S. Goulding, IEEE Trans. Nucl. Sci., 29: 619 (1982).

17. F. S. Goulding and D. A. Landis, IEEE Trans. Nucl. Sci., 29: 1125 (1982).

18. J. Llacer, E. E. Haller, and R. C. Cordi, IEEE Trans. Nucl. Sci., 24: 53 (1977).

19. F. S. Goulding, Nucl. Instr. and Meth., 142: 213 (1977).

20. D. D. Cohen, Nucl. Instr. and Meth., 178: 481 (1980).

21. I. M. Szoghy, J. Simon, and L. Kish, X-Ray Spec., 10: 168 (1981).

22. J. L. Campbell and P. L. McGhee, Nucl. Instr. and Meth. in Phys. Res., A248: 393 (1986).

23. F. S. Goulding, J. M. Jaklevic, B. V. Jarrett, and D. A. Landis, Adv. X-Ray Anal., 15: 470 (1972).

24. J. M. Jaklevic and F. S. Goulding, IEEE Trans. Nucl. Sci., 19: 384 (1972).

25. D. A. Gedcke, X-Ray Spec., 2: 129 (1972).

26. P. J. Statham, X-Ray Spec., 6: 95 (1977).

27. J. M. Hayes, D. E. Matthews, and D. A. Schoeller, Anal. Chem., 50: 25 (1978).

28. J. M. Jaklevic, D. A. Landis, and F. S. Goulding, Adv. X-Ray Anal., 19: 253 (1976).

29. J. E. Stewart, H. R. Zulliger, and W. E. Drummond, Adv. X-Ray Anal., 19: 153 (1976).

30. H. Thiebeau, J. Stadel, W. Cline, and T. A. Cahill, Nucl. Instr. and Meth., 111: 615 (1973).

31. P. J. Statham, G. White, J. V. P. Long, and K. Kandiah, X-Ray Spec., 3: 153 (1974).

32. H. J. Winick and S. Doniach, eds., Synchrotron Radiation Research, Plenum Press, New York (1980).

33. D. J. Bloomfield, G. Love, and V. D. Scott, X-Ray Spec., 12: 2 (1983).

34. J. M. Hayes, D. E. Matthews, and D. A. Schoeller, Anal. Chem., 50: 25 (1978).

35. J. M. Jaklevic, J. T. Walton, R. E. McMurray, Jr., N. W. Madden, and F. S. Goulding, "Semiconductor Detector Performance for Low-Energy X-Rays," Proceedings of Synchrotron Radiation Instrumentation 5th National Conf, Madison, WI, to be published in Nucl. Instr. and Meth. (1988).

36. R. G. Musket, Nucl. Instr. and Meth., 117: 385 (1974).

37. C. E. Cox, B. G. Low, and R. A. Sarren, Proceedings of the 1987 IEEE Nucl. Sci. Symposium, to be published in IEEE Trans. Nucl. Sci. (Feb. 1988).

38. B. Skillicorn, Adv. X-Ray Anal., 25: 49 (1982).

39. M. Green and V. E. Cosslett, Proc. Phys. Soc. (London), 78: 1206 (1961).

40. R. Tertian and N. Broll, X-Ray Spec., 13: 135 (1984).

41. R. C. Placious, J. of Appl. Phys., 38: 2030 (1967).

42. J. M. Jaklevic, R. C. Gatti, F. S. Goulding, B. W. Loo, and A. C. Thompson, Environmental Protection Agency Technical Report No. EPA-60/4-78-034 (May, 1980).

43. M. C. Nichols, D. R. Boehme, R. W. Ryon, D. Wherry, B. Cross, and G. Aden, Adv. X-Ray Anal., 30: 45 (1987).

44. W. Michaelis, J. Knoth, A. Prange, H. Schwenke, Adv. X-Ray Anal., 28: 75 (1985).

45. H. Aiginger and P. Wobrovschek, Adv. X-Ray Anal., 28: 1 (1985).

46. R. W. Ryon, J. D. Zahrt, P. Wobrauschek, and H. Aiginger, Adv. X-Ray Anal., 25: 633 (1982).

47. C. Ruch, F. Rastegar, R. Heimburger, E. A. Maier, and M. J. F. Leroy, Anal. Chem., 57: 1691 (1985).

48. C. L. Luke, Anal. Chim. Acta, 41: 237 (1968).

49. A. T. Ellis, D. E. Leyden, W. Wegscheider, B. B. Jablonski, and W. B. Bodnar, Anal. Chim. Acta, 142: 73 (1982).

50. W. J. Campbell, F. Spano, and T. E. Green, Anal. Chem., 38: 987 (1966).

51. H. Kingston and P. A. Pella, Anal. Chem., 53: 223 (1981).

52. D. E. Leyden and W. Wegscheider, Anal. Chem., 53: 1059A (1981).

53. R. Van Greiken, Anal. Chim. Acta, 143: 3 (1982).

54. P. J. Potts, P. C. Webb, and J. S. Watson, X-Ray Spec., 13: 2 (1984).

55. R. D. Giauque, R. B. Garrett, and L. Y. Goda, Anal. Chem., 51: 511 (1979).

Figure Captions

1) Basic elements in EDXRF measurements. a) The exciting radiation creates vacancies in the inner shells of the sample atoms. The characteristic x-rays which are emitted are observed by the energy dispersive detector. b) A schematic of the fluorescence process.
2) Cross section of a typical Si(Li) detector showing evaporated electrode contacts and active volume. HPGe differs in that the bulk is formed by high purity Ge which does not require the compensation of electrically active centers by lithium drifting.
3) Pulse height spectrum of Mn K x-rays obtained with a Si(Li) energy dispersive detector. The pulser peak is acquired simultaneously as an indicator of the electronic component to energy resolution.
4) Simplified schematic diagram of a typical pulse processing system used for energy dispersive detectors.
5) Relative contribution of electronic noise sources to the total electronic resolution as a function of the characteristic time constant of the pulse shaper. N_s2 is the component associated with fluctuations in the detector leakage current; $N\Delta 2$ is due to leakage currents in subsequent amplification stages. The dashed curve is the sum of the two.
6) Calculated total energy resolution vs. incident photon energy for both Si and Ge detectors. Asymptotic values show resolution limits assuming no contribution due to electronics processing.
7) Calculated photopeak efficiency for Si and Ge detectors as a function of incident photon energy. The high energy limits are

established by the photoelectric cross section of the detector material and the diode thickness. Low energy cutoff is determined either by absorption in the thin Be window or in a nominal 2 cm air path from source to detector.

8) Schematic spectrum calculated assuming 17 keV excitation on a carbon matrix with a typical contribution to the background due to incomplete charge collection. Peak heights of elements are calculated assuming equal mass concentrations for each. Variation in intensity is due to decrease in excitation efficiency of monoenergetic excitation for lighter elements.

9) Time sequence of pulses which occur during the processing of a series of x-ray events. Curve (A) shows the output of the preamplifier represented as a series of voltage steps reflecting the integrated charge from the individual events. (B) is the output from a fast shaping amplifier which operates with a shorter time constant than the main shaping system. (C) is a fast discriminator timing pulse derived from (B). The output of the main shaper is shown in (D) with the pileup of pulses 2 and 3 indicated. (E) shows the dead-time gates and (F) the final output with the ambiguous 2 and 3 pile-up pulses rejected.

10) Non-pileup output rate as a function of input rate scaled as a function of a characteristic shaping time. Maximum output is 0.37 of the input rate equal to the reciprocal of the time constant.

11) Calculated efficiencies for the very low energy region showing the limits to efficiency determined by the entry window of the detector itself. Curves a) and b) show the absorption due to either an

evaporated Al or Au layer of typical thicknesses required for contacts. Curves c)and d) show the effect of an "intrinsic" Si or Ge window.

12) Schematic diagram of an x-ray tube and typical excitation geometries. The high energy electron beam strikes the anode to produce x-rays. The flux (1) is either used directly to strike target (1). In the second case, beam (1) strikes a secondary target which generates a second flux of x-rays which strikes the sample. In the third case, the direct beam (3) is directed through the anode in a transmission geometry.

13) Schematic spectrum of x-rays emitted from a Mo anode operated at 60 keV.

14) Calculated probability for characteristic production of x-rays as a function of target atomic number for three choices of incident characteristic x-rays: Cu k-alpha at 8.0 keV, Mo k-alpha at 17.4 keV and Tb k-alpha at 44.2 keV.

15) Plot of x-ray fluorescence spectrum obtained using a Mo secondary target excitation of a atmospheric aerosol sample.

16) Spectrum of aerosol sample shown in Figure 15 but acquired with a Sm excitation. The Ta lines in the low energy region are due to excitation of the collimator. Note the order of magnitude difference in vertical scale.

17) Spectrum obtained from a NBS SRM 1634 liquid fuel oil sample using Mo excitation.

TABLE 1. Detector Properties of Silicon and Germanium[a)]

	Si	Ge
Atomic Number	14	32
Atomic Weight	28.09	72.60
Density (300 K); g/cm^3	2.33	5.33
Band Gap (300 K); eV	1.115	0.665
Average Energy (ϵ) per Hole-Electron Pair (77 k); eV	3.76	2.96
Fano Factor (77 K)	0.12	0.08

a) Adapted from Ref. 7.

TABLE 2. X-Ray Tube Anode Characteristics

Anode Material	Characteristic Radiation and Energy (keV)		Anode[a)] Voltage kV	Approximate[b)] X-Ray Yield
Cr	K	5.4	18	2.0×10^{-4}
Cu	K	8.0	27	2.2
Mo	K	17.4	60	2.2
Rh	K	20.1	66	2.3
Ag	K	22.1	75	2.4
W	L*[c)]	8.4, 9.7	30*	1.5
Au	L*[c)]	9.7, 11.4	40*	1.5

a) Anode voltage assume V = 3 x K or L absorption edge energy.

b) Expressed as total k-quanta per electron per steradian. Adapted from Ref. 39.

c) The high z transits are often chosen because of the intense continuum radiation available. In these cases higher anode voltages may be desirable.

TABLE 3. Elemental Concentrations in NBS SRM 1571 Orchard Leaves ($\mu g/g \pm 2\sigma$)

Element	XRF	NBS
Ti	18.0 ± 8.5	---
V	< 8	---
Cr	< 5	2.6 ± 0.3
Mn	86.5 ± 4.9	91 ± 4
Fe	274 ± 19	300 ± 20
Co	< 6	(0.2)
Ni	1.2 ± 0.5	2.3 ± 0.2
Cu	11.5 ± 1.0	12 ± 1
Zn	25.3 ± 2.1	25 ± 3
Ga	< 0.5	---
Ge	< 0.4	---
As	10.1 ± 0.8	10 ± 2
Se	< 0.3	0.08 ± 0.01
Br	9.0 ± 0.5	(10)
Rb	11.5 ± 0.6	12 ± 1
Sr	36.3 ± 1.3	(37)
Y	< 1	---
Zr	< 3	---
Hg	< 1	0.155 ± 0.015
Pb	40.7 ± 3.0	45 ± 3
Th	< 1	---
U	< 2	0.029 ± 0.005

TABLE 4. Minimum detection limits (ng/cm^2) for Teflon filters in helium atmosphere.

X-ray tube voltage (KV)	50		60		70	
Secondary target	Ti		Mo		Sm	
Time interval (min)[a]	2		3		4	
	Element	MDL	Element	MDL	Element	MDL
	Al	130	Ti	30	Zr	8
	Si	45	V	20	Mo	5
	S	15	Cr	16	Ag	5
	Cl	13	Mn	12	Cd	6
	K	6	Fe	12	In	6
	Ca	5	Ni	5	Sn	8
			Cu	6	Sb	8
			Zn	5	Te	10
			Ga	4	I	13
			Ge	3	Cs	24
			As	4	Ba	40
			Se	2		
			Br	2		
			Rb	3		
			Sr	3		
			Hg	7		
			Pb	8		

a) All three runs were normalized to an equivalent amount of integrated current in the pulsed x-ray tube.

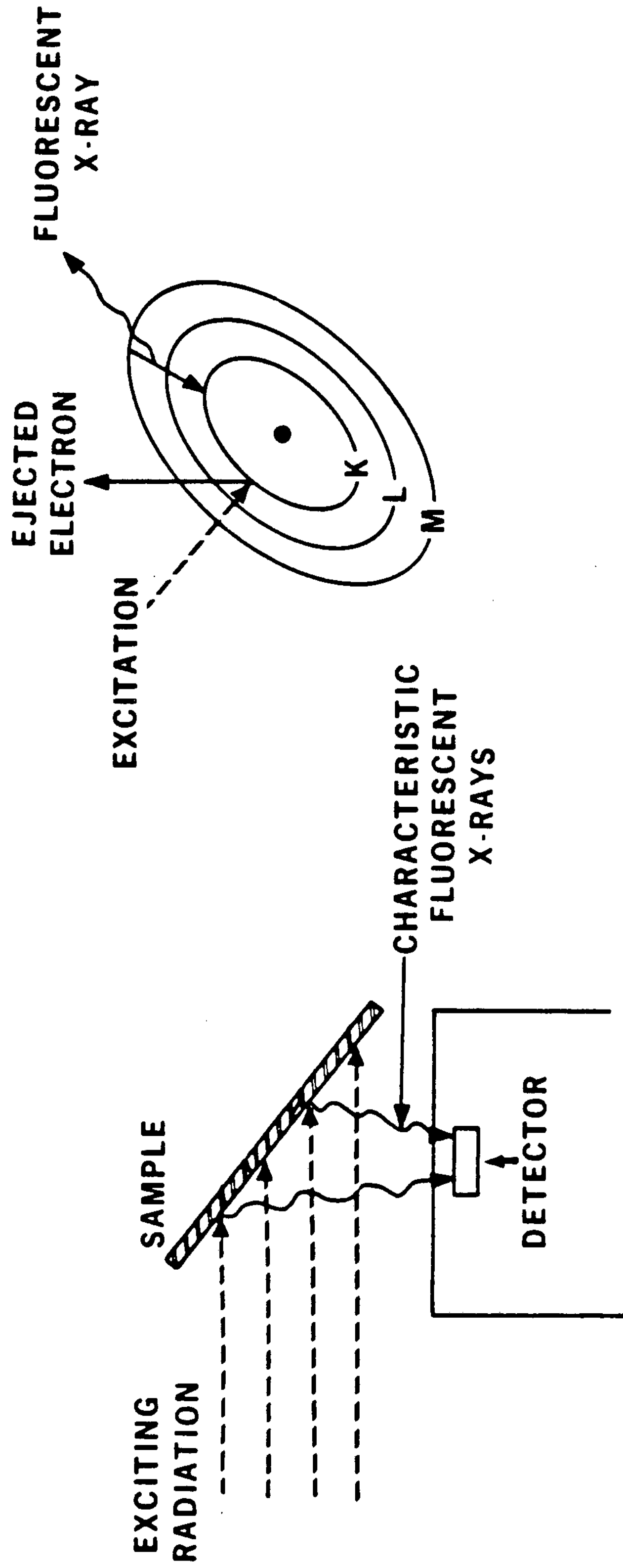

Fig. 1.

XBL 733-287

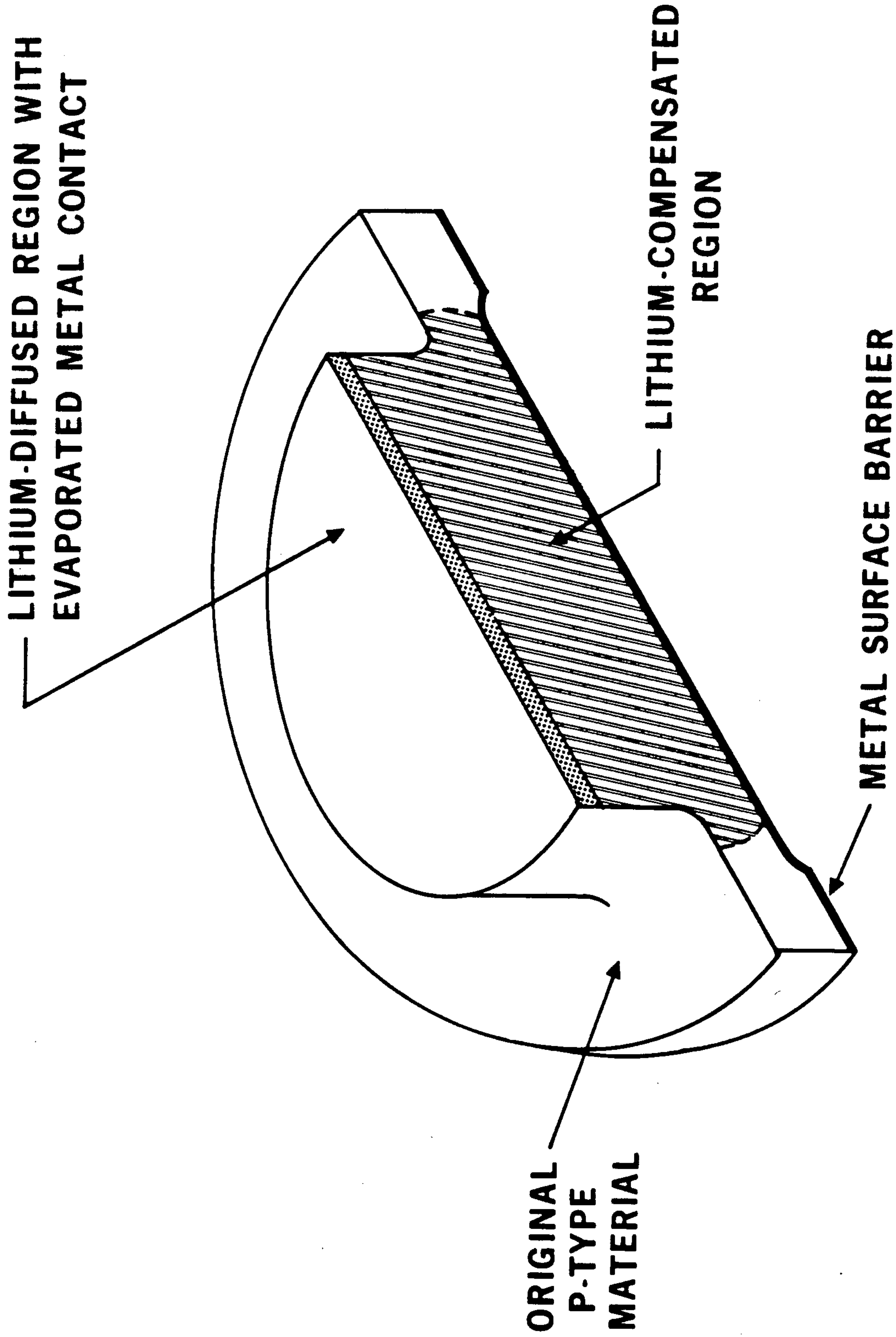

Fig. 2.

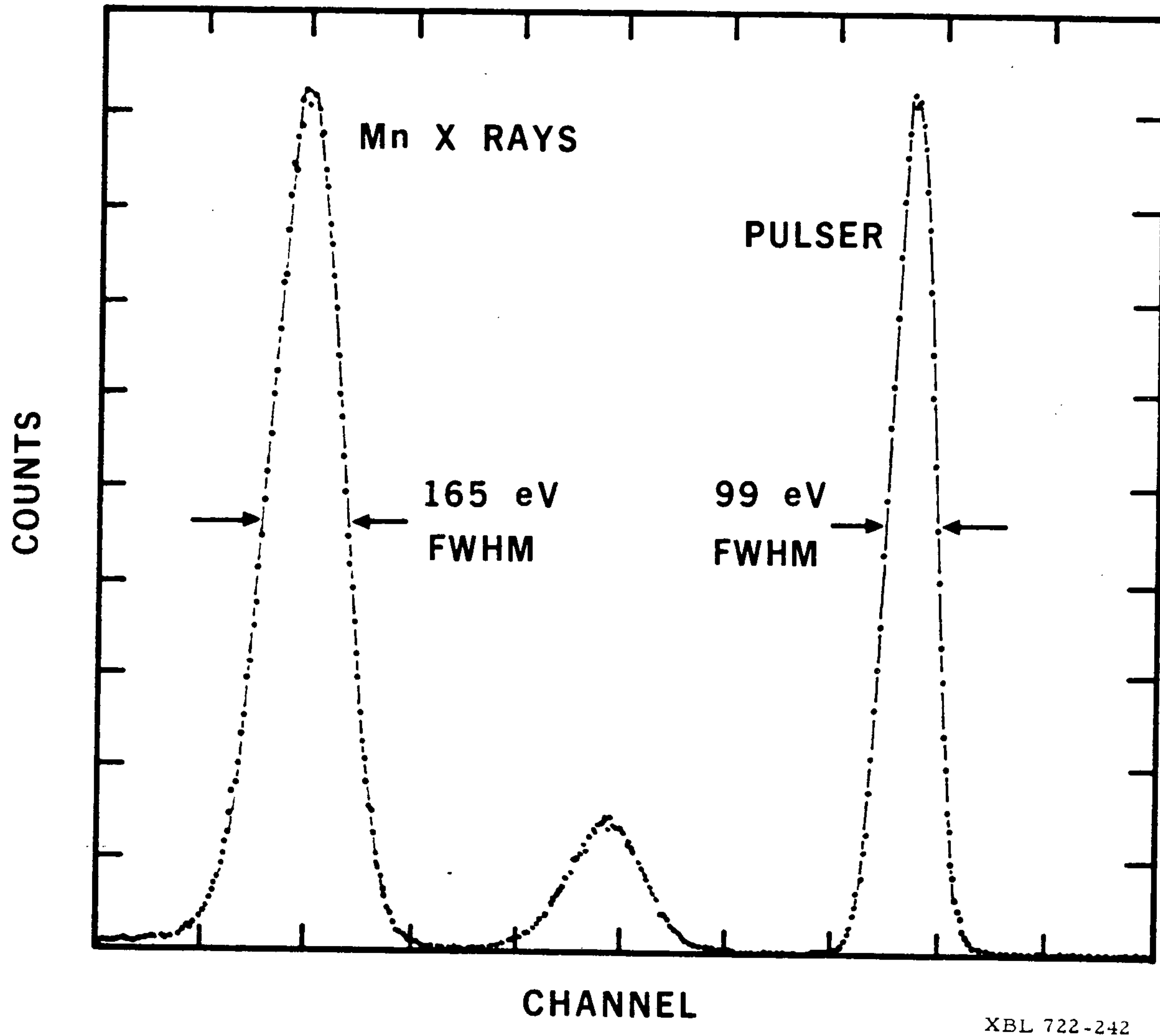

Fig. 3.

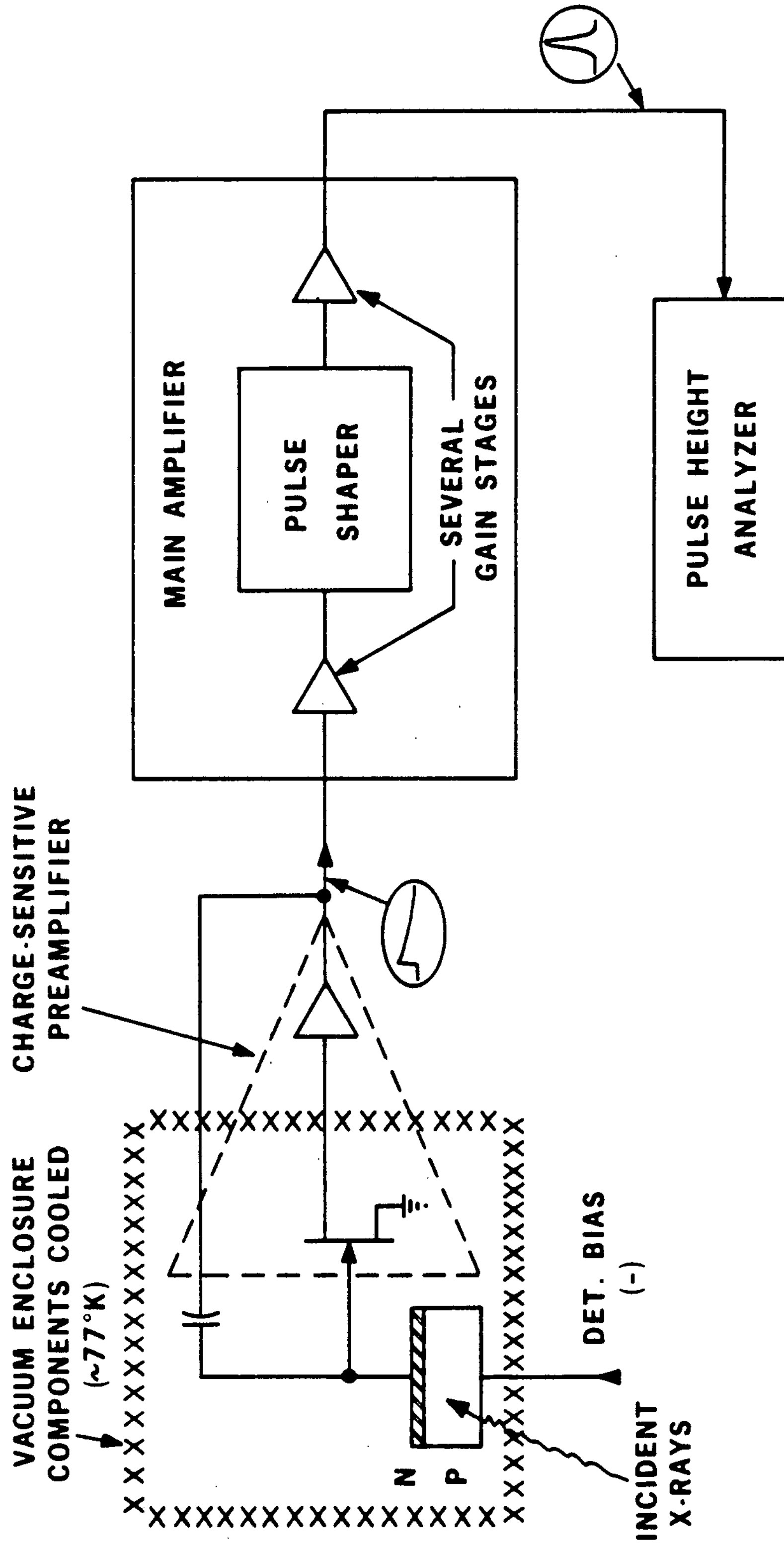

XBL 733-284

Fig. 4.

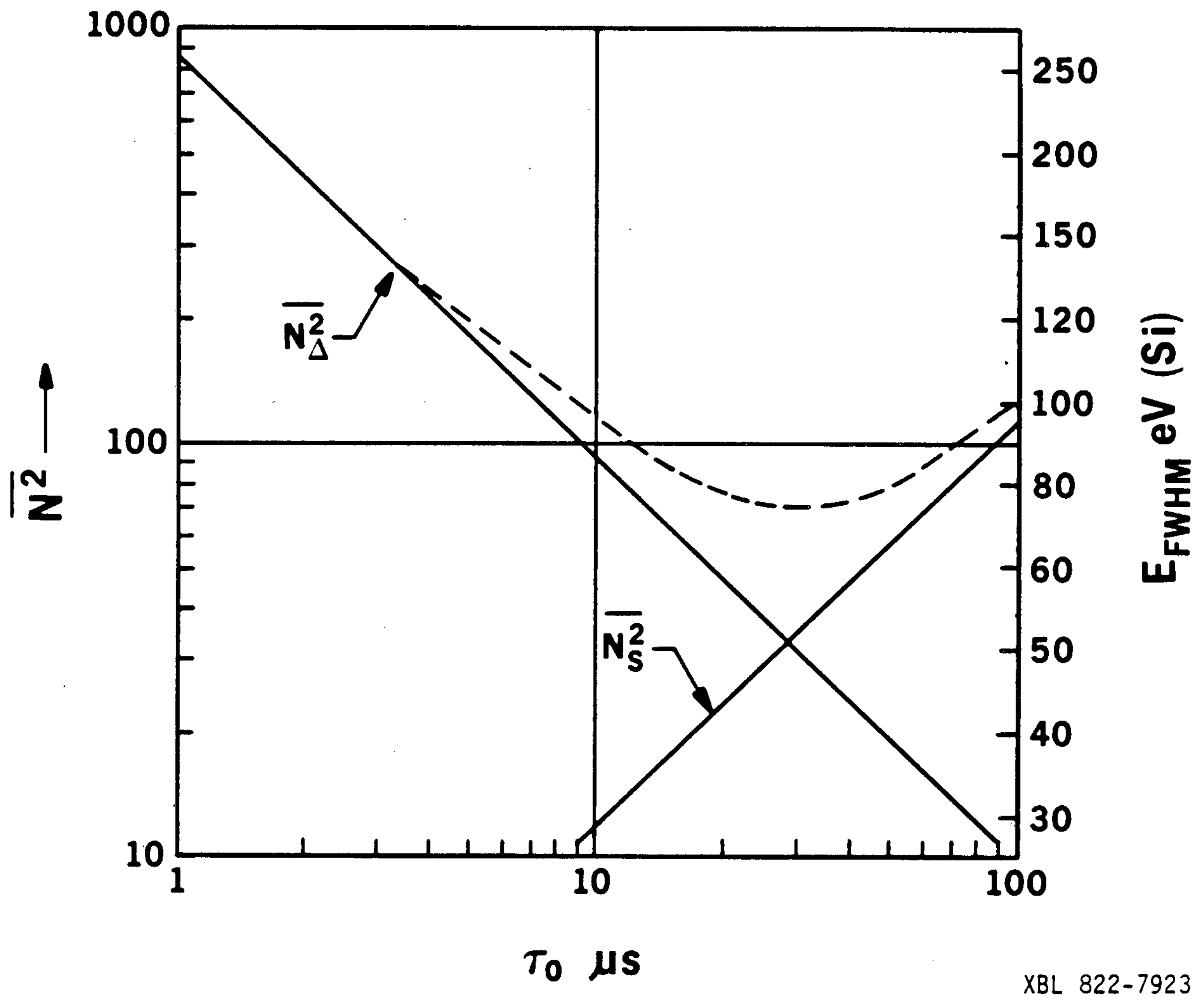

Fig. 5.

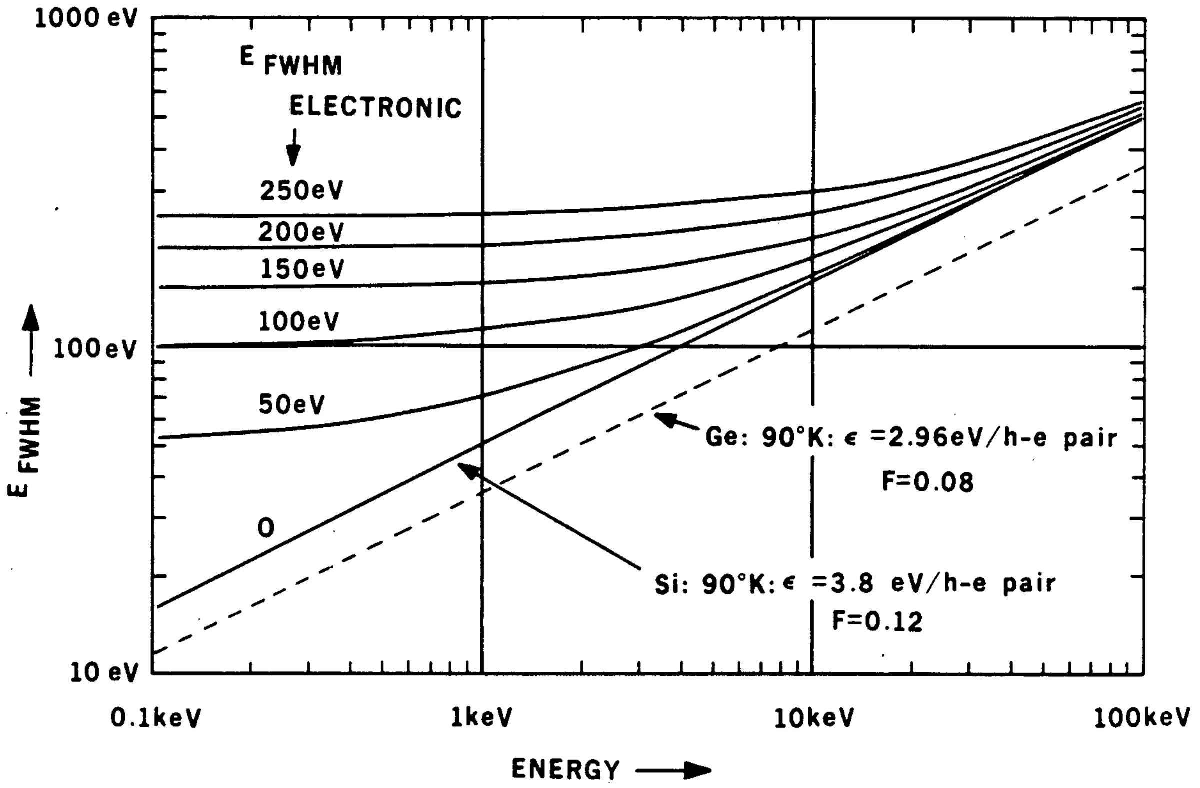

XBL 724-788

Fig. 6.

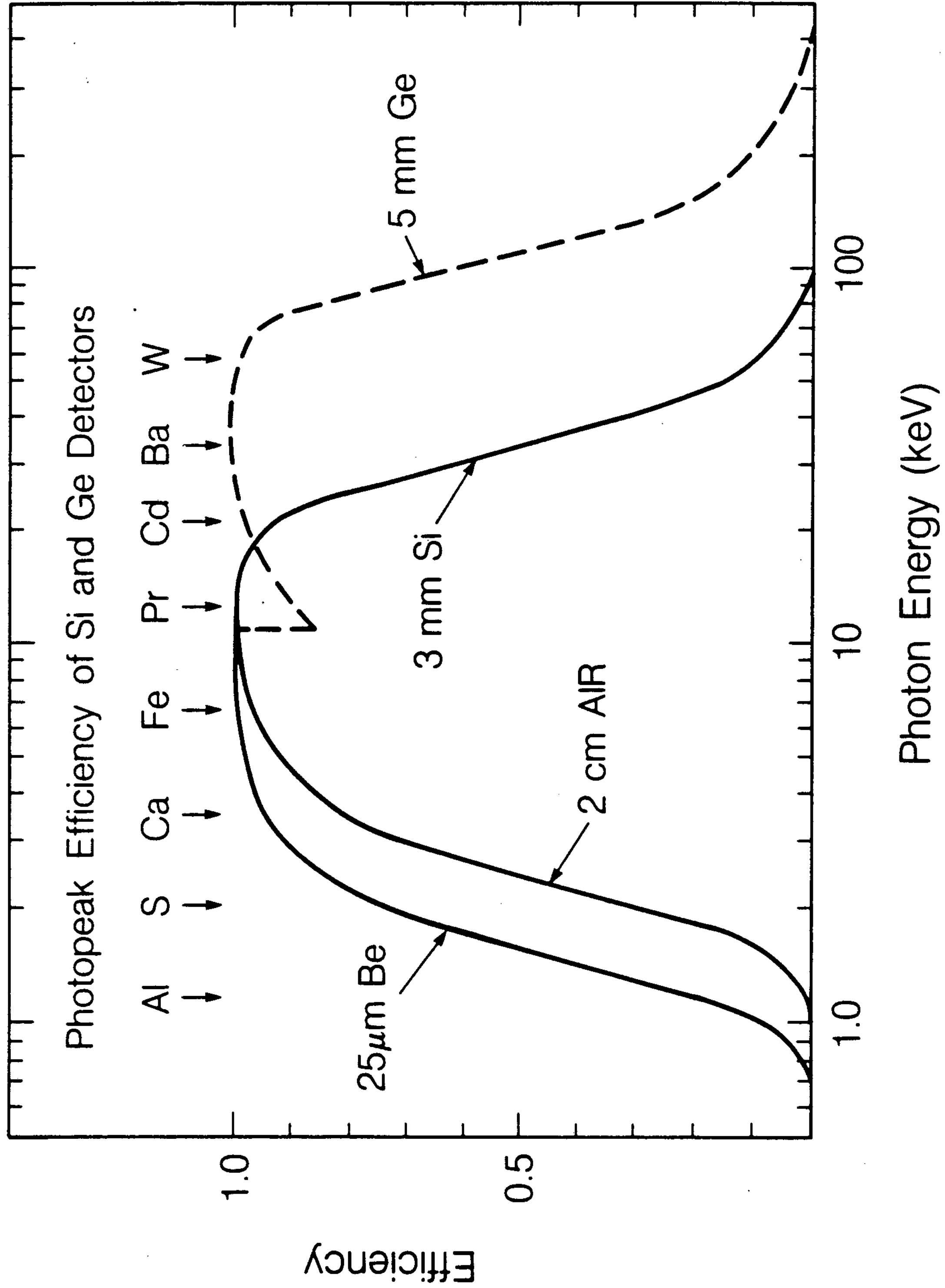

XBL 881-10030

Fig. 7.

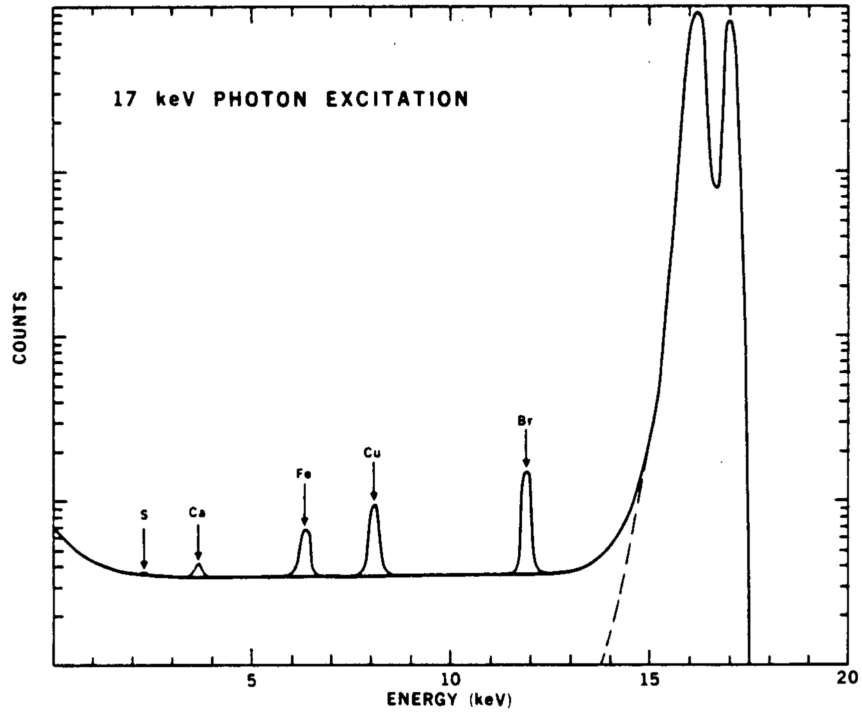

Fig. 8.

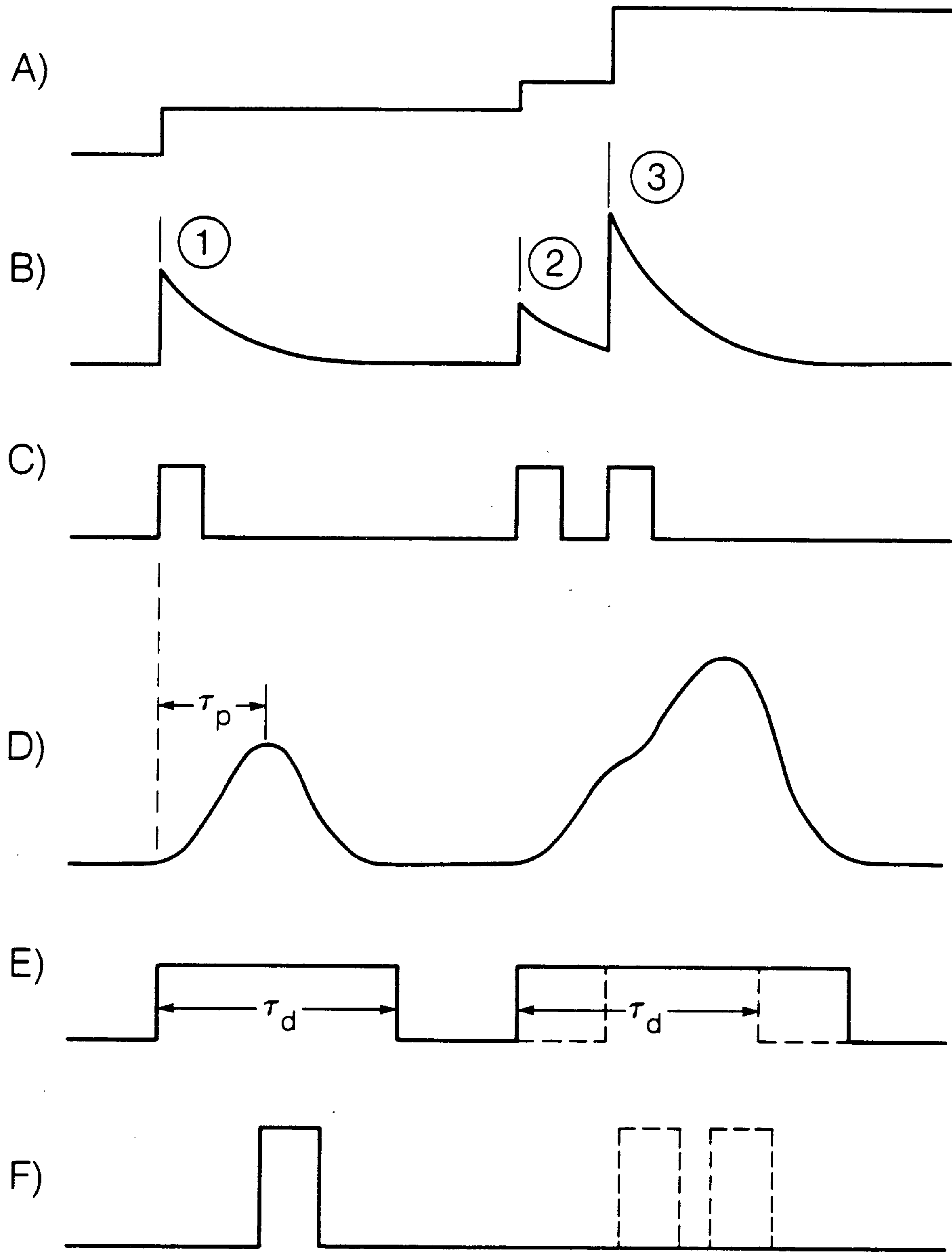

Fig. 9.

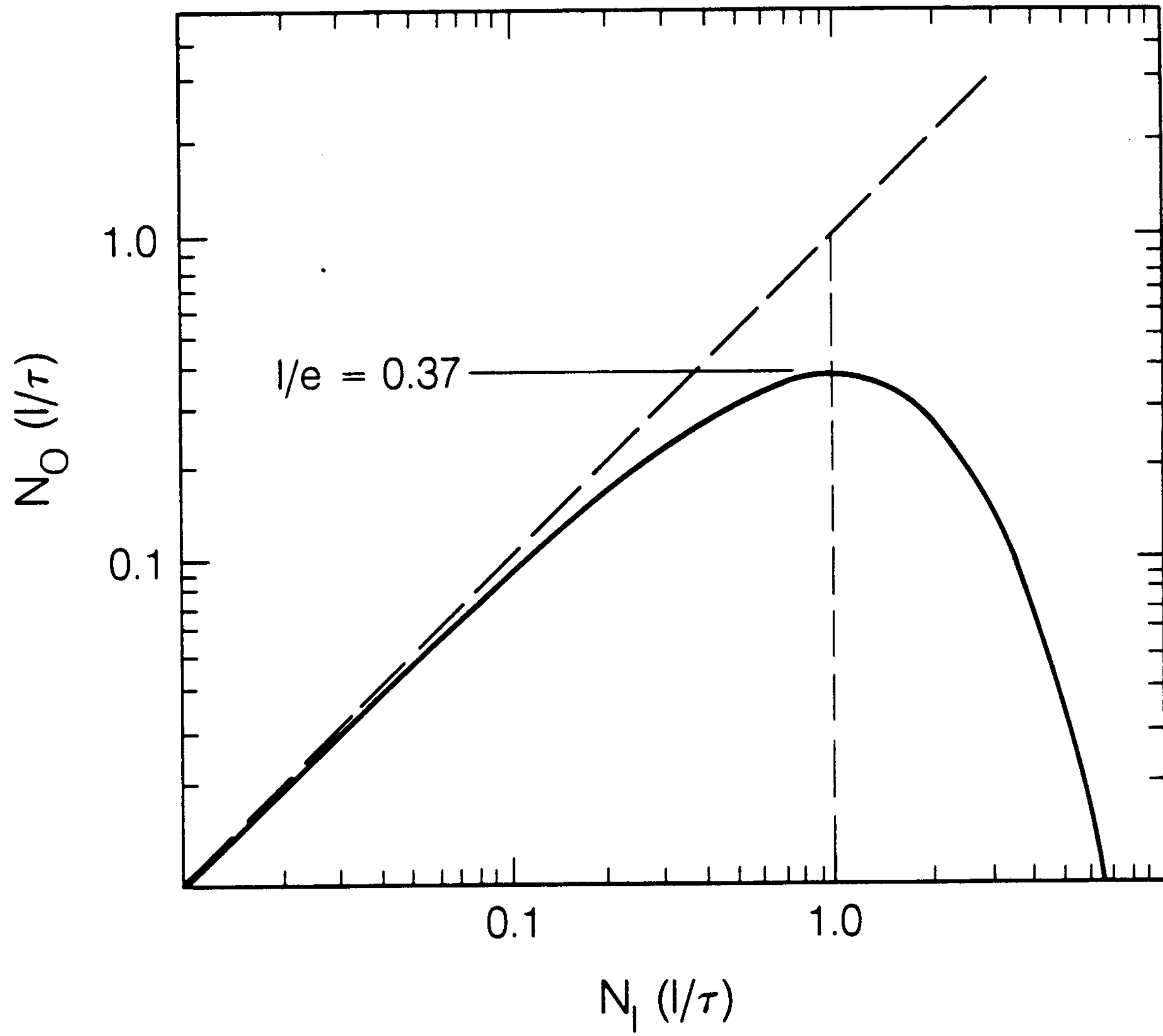

XBL 881-10031

Fig. 10.

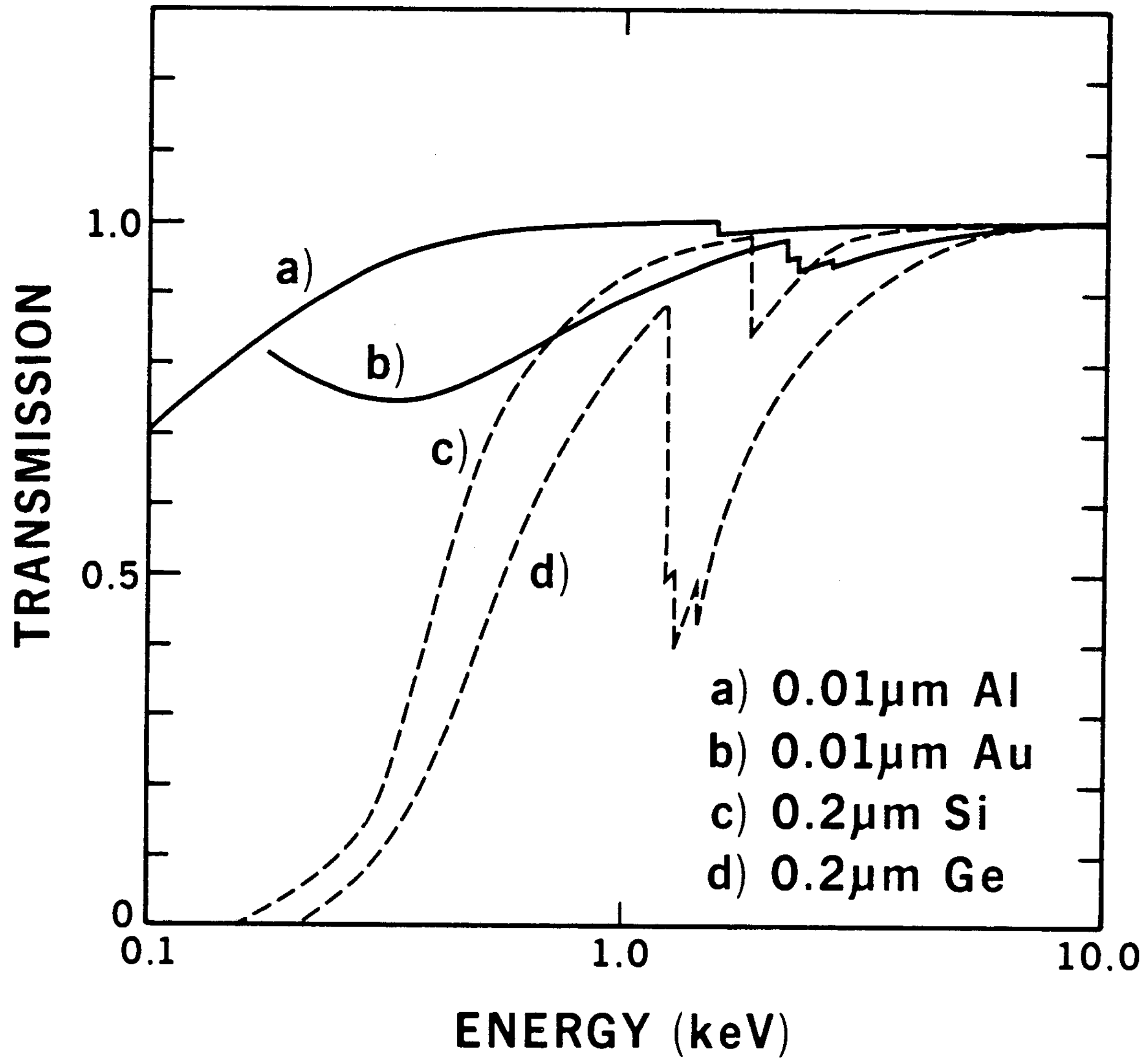

XBL 876-2838

Fig. 11.

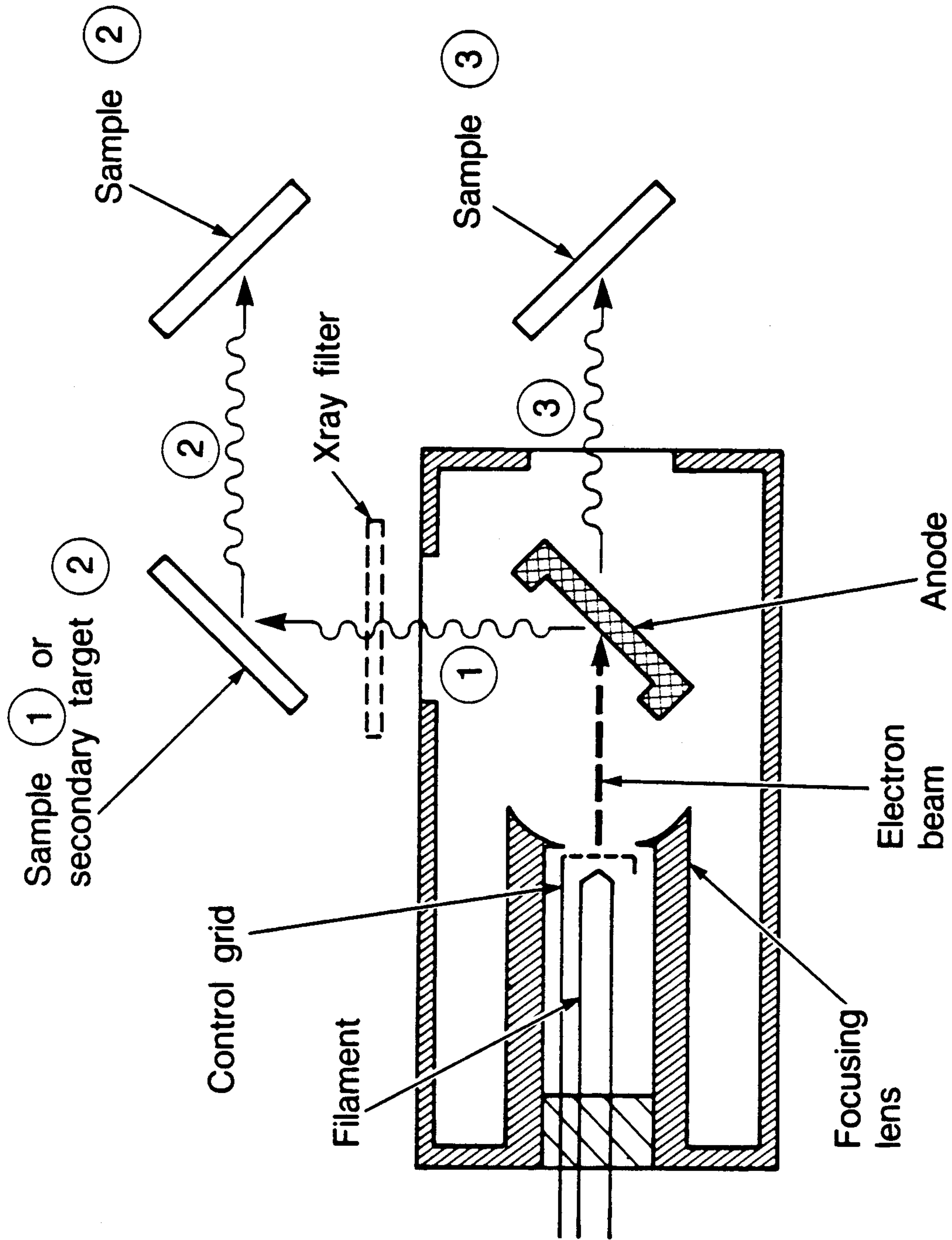

Fig. 12.

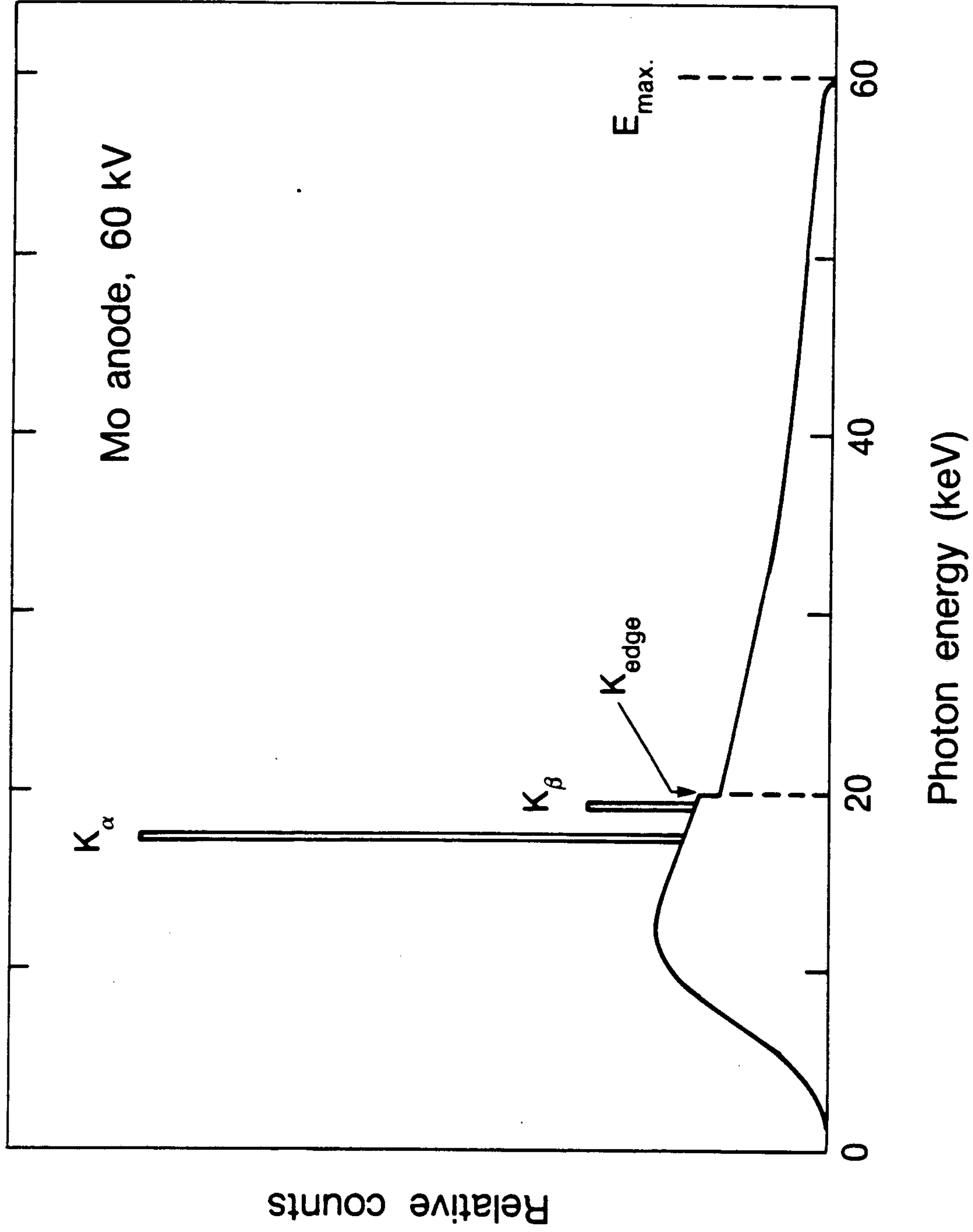

Fig. 13.

XBL 882-9547

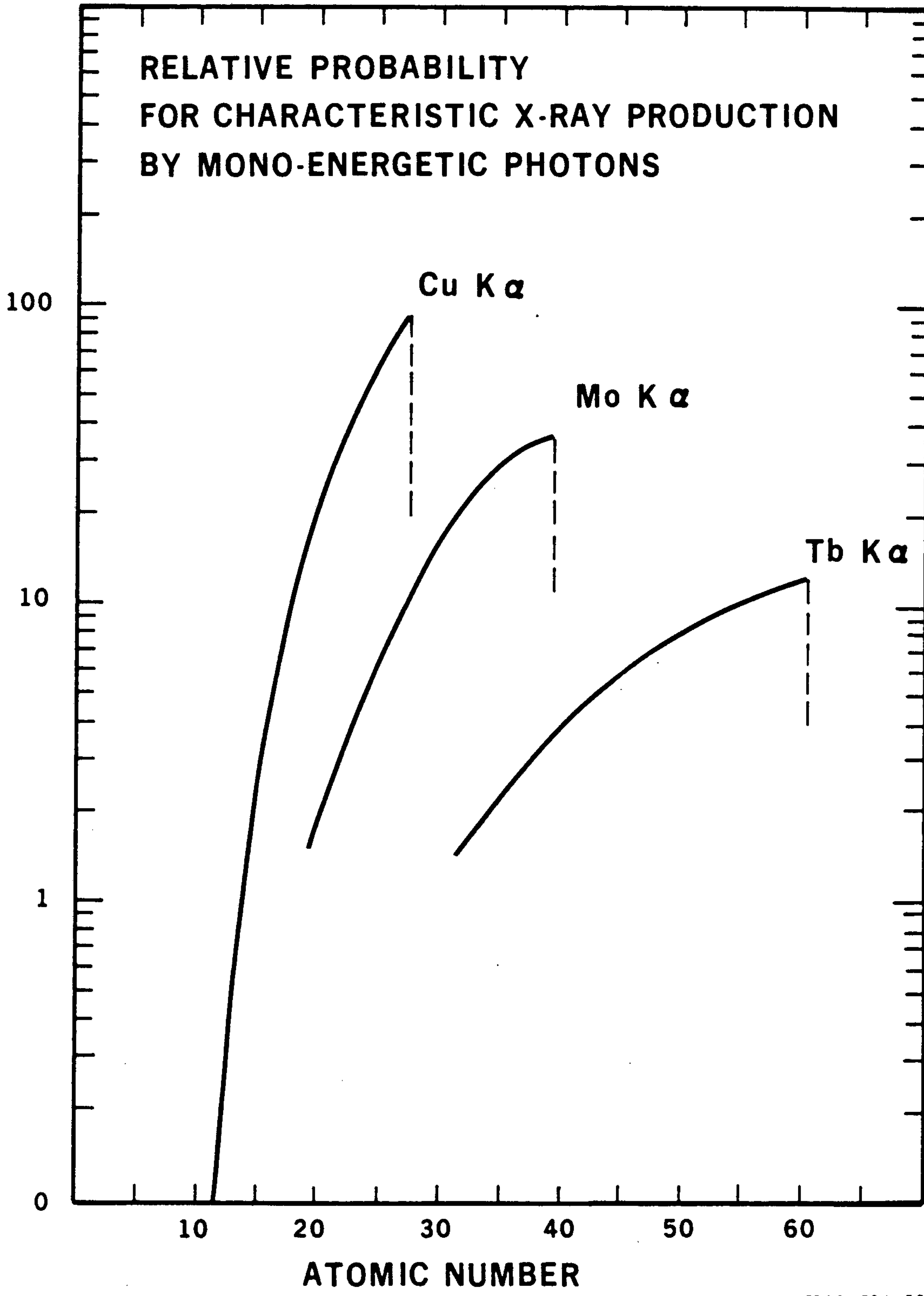

Fig. 14.

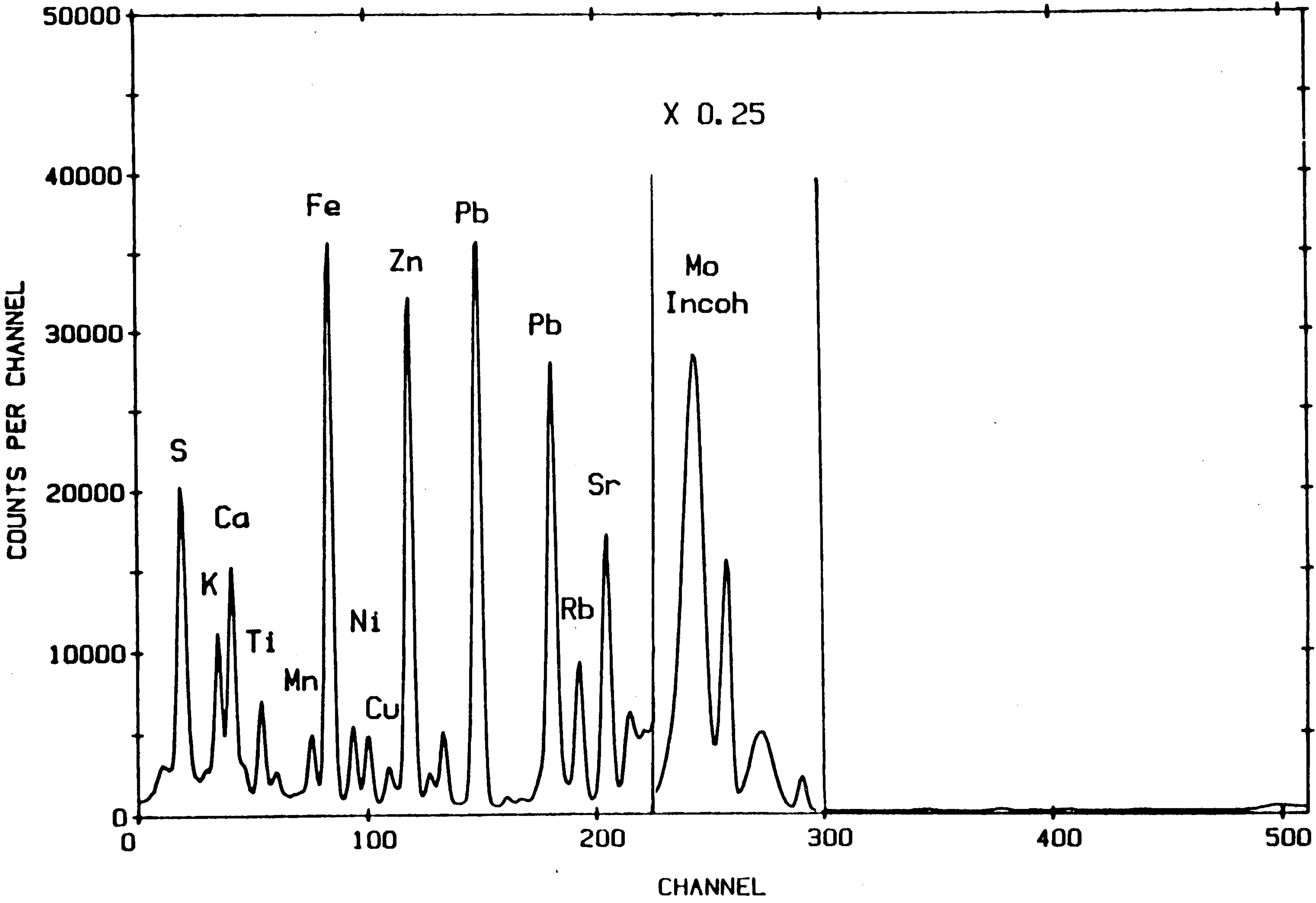

Fig. 15.

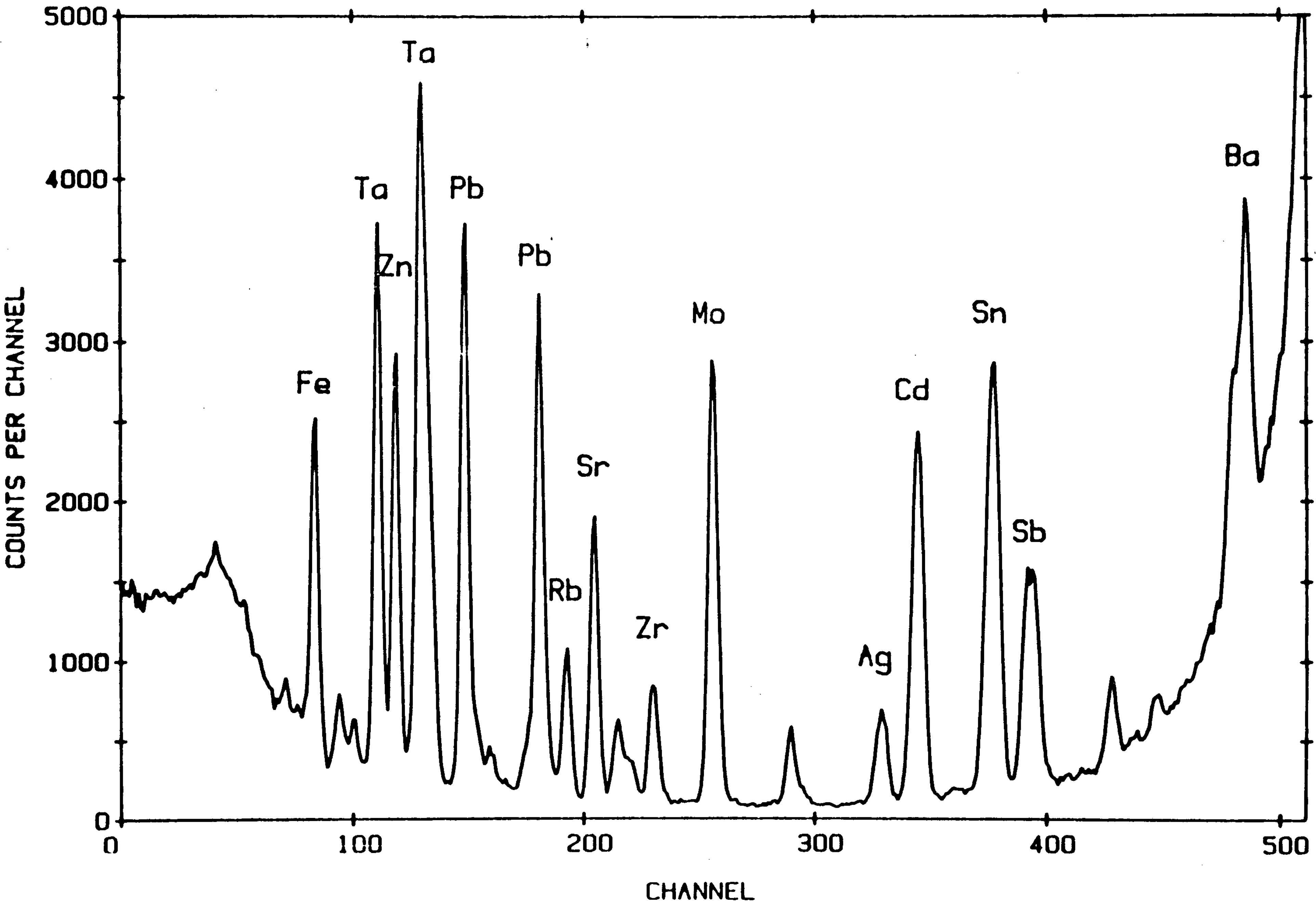

Fig. 16.

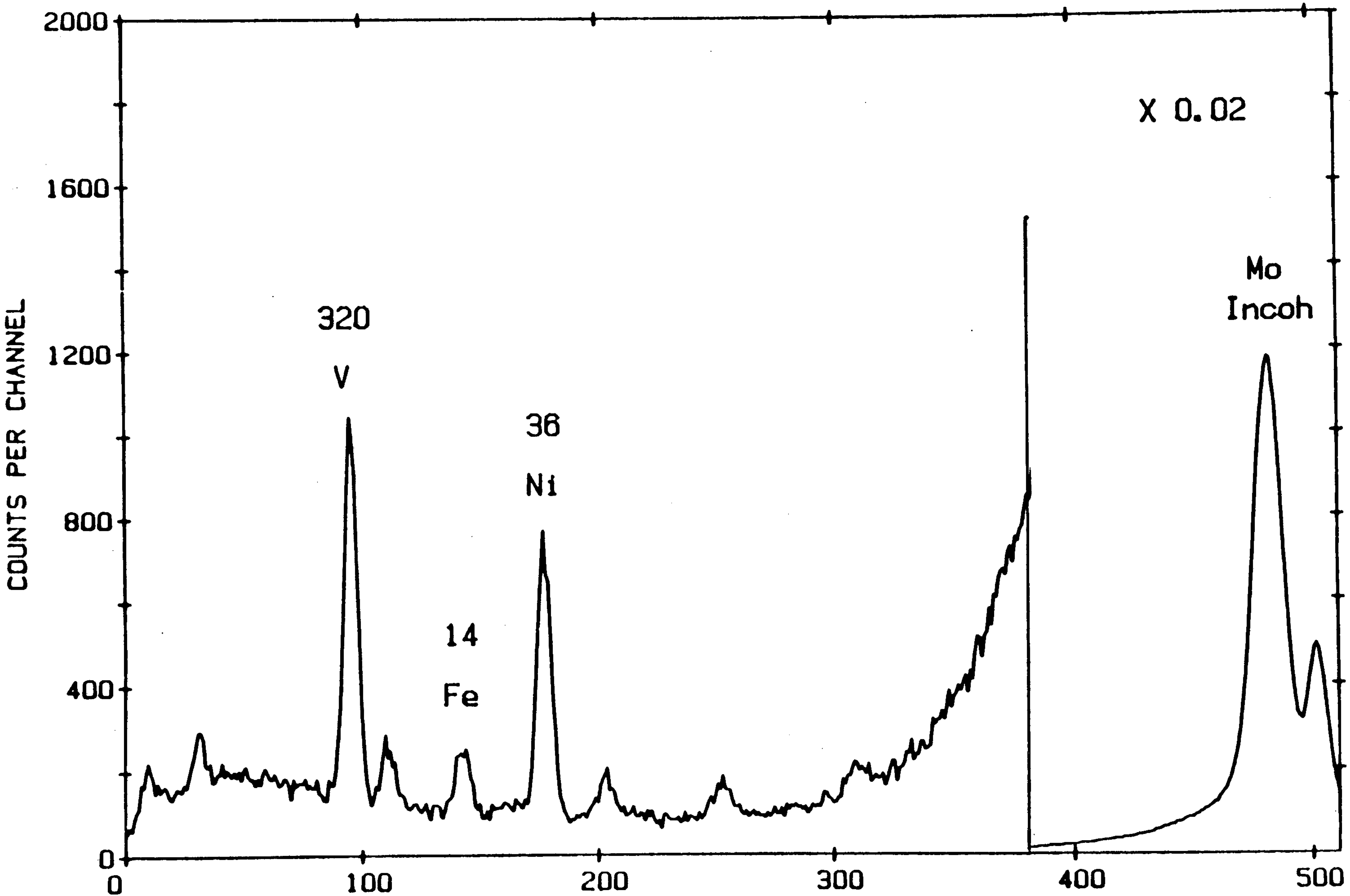

Fig. 17.

LAWRENCE BERKELEY LABORATORY
TECHNICAL INFORMATION DEPARTMENT
UNIVERSITY OF CALIFORNIA
BERKELEY, CALIFORNIA 94720